ACS OMEGA

Open Access

http://pubs.acs.org/journal/acsodf

Article

Ferrocenyl-Substituted Curcumin Derivatives as Potential SHP-2 Inhibitors for Anticolorectal Cancer: Design, Synthesis and *In Vitro* Evaluation

Xing-Ze Zhang,[#] Gen Li,[#] Gao-Yong Hu,[#] Chen-Lin Wang, Yu-Qiu Fang, Yuye Li,* Xue-Jie Qi,* and Lili Duan*

Cite This: *ACS Omega* 2024, 9, 51701−51718

Read Online

ACCESS | Metrics & More | Article Recommendations | Supporting Information

ABSTRACT: A panel of ferrocenyl-substituted curcumin derivatives has been designed and synthesized as protein tyrosine phosphatase proto-oncogene SHP-2 inhibitors. Antiproliferative activities of the synthesized compounds were tested against colorectal cancer cell lines (including RKO, SW480, and CT26). Compound **3f** showed excellent activities against the tested cell lines with IC_{50} values of 5.72, 3.71, and 1.42 μM. The cytotoxicity of compound **3f** was investigated on human normal colon epithelial cell line NCM460 with IC_{50} values of 929 μM compared to curcumin with IC_{50} values of 431 μM. The Western blot analysis approved that the expression level of SHP-2 in the CT26 and SW480 cell lines after being treated with **3f** was decreased, meanwhile it also affected the SHP-2 in tumor-associated macrophages (THP-1 and RAW264.7), which may support the suggested mechanism of **3f** as an SHP-2 inhibitor. Besides, **3f** could also inhibit the activation of the PI3K-Akt pathway in SW480 and CT26 cell lines and the tumor microenvironment (TME) by reducing the expression of PI3K and Akt proteins. Some cytokines (Arg-1, TGF-β, and IL-10) and chemokines (chemokine receptors and CC and CXC chemokine subfamilies) in the TME were also inhibited by **3f**. Finally, **3f** could increase the expression level of cell cycle-related and mitophagy-related proteins p27, PINK1, and Parkin and decrease the expression level of CDK1 and Cyclin-D1 proteins in CT26 and SW480 cells, which proved that **3f** could inhibit the proliferation of CRC cells through multiple pathways. Molecular docking studies against ALDH1 (PDB ID: 5ABM) revealed the good binding modes of the newly synthesized compounds.

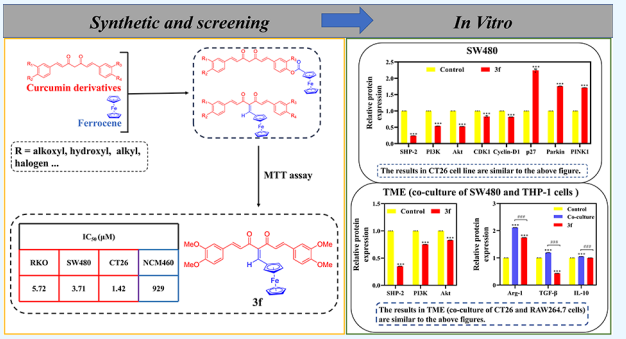

1. INTRODUCTION

Inflammation has been established to be closely linked to cancer development.[1] If the acute inflammatory response fails to resolve promptly, it can evolve into chronic inflammation, resulting in an immunosuppressive microenvironment characterized by the substantial presence of immunosuppressive cells and cytokines. This state can lead to the suppression of T cell functionality, consequently promoting tumor formation.[2] In the context of chronic inflammation, tumor-associated macrophages (TAMs) are stimulated by M1-TAMs to M2-TAMs, which perpetuates an immunosuppressive state within the tumor microenvironment (TME).[3]

Protein tyrosine phosphatase (PTP) is intricately linked to cellular proliferation, differentiation, growth and apoptosis.[4] PTP is involved in numerous signal pathways associated with human diseases, including diabetes, obesity, and cancer; furthermore, its role in tumor development and transformation has attracted increasing attention.

SHP-2, Src homology region 2 domain-containing protein tyrosine phosphatase-2, is encoded by the PTPN11 gene.[5] As a potential target for anticolorectal cancer (CRC) therapy and immunosuppression,[6] SHP-2 is involved in various signal pathways, including PI3K/Akt in tumor cells, and may promote tumor initiation and progression.[7] Furthermore, SHP-2 is regarded as a promising target for modulating TAM function in cancer immunotherapy, as it can facilitate the polarization of M1-TAMs.[8] Consequently, the inhibition of SHP-2 is crucial, as it can restrain tumor cell proliferation, overcome targeted drug resistance, and activate the immune system.

Given SHP-2's role in promoting various malignant behaviors of tumor cells, the development of molecular inhibitors, particularly allosteric inhibitors, has garnered significant attention. To date, three allosteric inhibitors—

Received: November 22, 2024
Revised: December 6, 2024
Accepted: December 12, 2024
Published: December 18, 2024

TNO155,[9,10] RMC-4630,[11,12] and JAB-3068[13−15] (Figure 1)—have been approved by the FDA for clinical trials.[16]

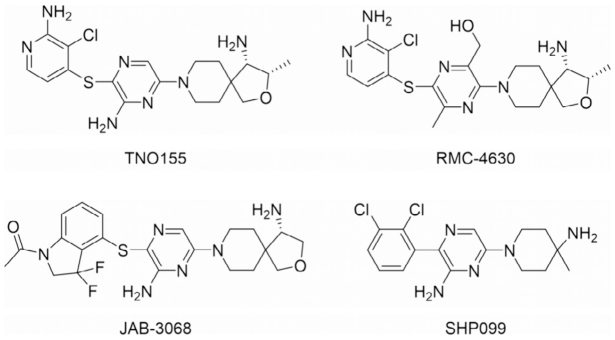

Figure 1. Inhibitors (TNO155, RMC-4630, JAB-3068, and SHP099) of SHP-2.

SHP099 is another highly efficient and selective SHP-2 inhibitor with an IC_{50} value of 0.071 μM, which can significantly inhibit the proliferation of cancer cells *in vitro*.[17]

Curcumin (Cur)[18] exhibits various pharmacological effects, including antitumor,[19] anti-inflammatory,[20] and antioxidant properties.[21] Numerous clinical trials have demonstrated that Cur can serve as a potential preventive or therapeutic agent for CRC.[22] It has been reported that Cur can enhance the binding of SHP-2 to janus kinase (JAK) by up-regulating the phosphorylation of SHP-2, which inhibits the phosphorylation of signal transducer and activator of transcription 3 (STAT-3) by JAK.[23,24] The JAK-STAT pathway is overactivated in various tumor cells, promoting tumor cell proliferation.[25] STAT-3 has the potential to promote cancer and is continuously expressed in numerous cancers.[26] Therefore, its inhibition may represent an effective strategy for controlling tumor development. Additionally, demethoxycurcumin (DMC), an analogue of Cur, can sustain the activation of the epidermal growth factor receptor (EGFR) by inhibiting

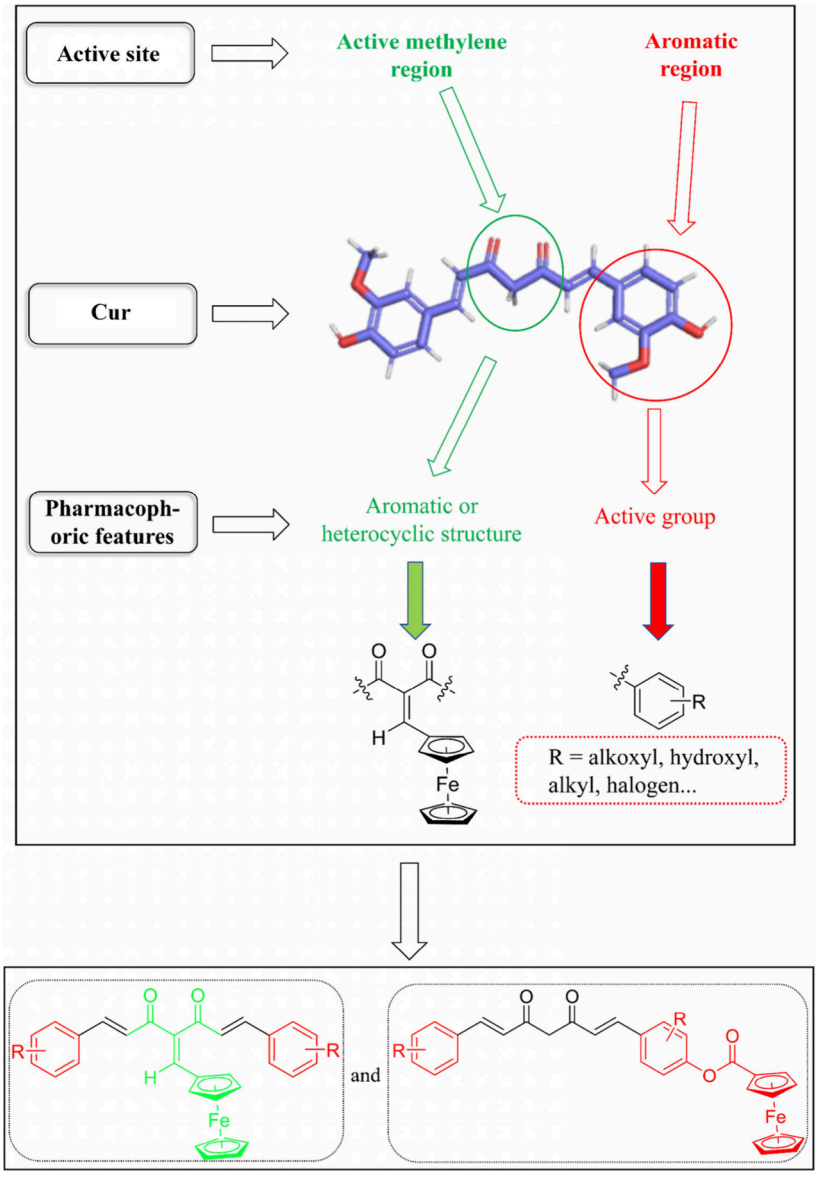

Figure 2. Design rationale of the ferrocenyl-substituted Cur derivatives.

https://doi.org/10.1021/acsomega.4c10629
ACS Omega 2024, 9, 51701−51718

Scheme 1. Preparation of Compounds 1a−1m[a]

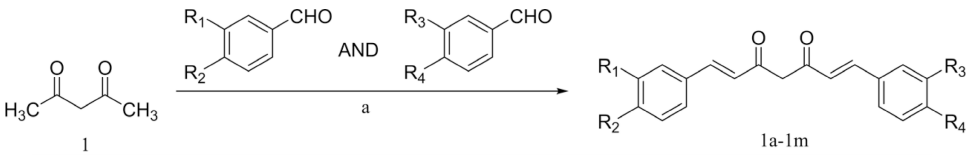

1a: R_1=OCH_3, R_2=OH, R_3=OCH_3, R_4=OH
1b: R_1=OCH_3, R_2=OCH_3, R_3=OCH_3, R_4=OH
1c: R_1=H, R_2=OH, R_3=H, R_4=OH
1d: R_1=OCH_3, R_2=OH, R_3=H, R_4=OH
1e: R_1=OCH_3, R_2=OCH_3, R_3=H, R_4=OH
1f: R_1=OCH_3, R_2=OCH_3, R_3=OCH_3, R_4=OCH_3
1g: R_1=CH_3, R_2=CH_3, R_3=CH_3, R_4=CH_3
1h: R_1=H, R_2=$CH(CH_3)_2$, R_3=H, R_4=$CH(CH_3)_2$
1i: R_1=H, R_2=$C(CH_3)_3$, R_3=H, R_4=$C(CH_3)_3$
1j: R_1=H, R_2=H, R_3=H, R_4=H
1k: R_1=H, R_2=Br, R_3=H, R_4=Br
1l: R_1=H, R_2=Cl, R_3=H, R_4=Cl
1m: R_1=H, R_2=F, R_3=H, R_4=F

[a]Reagents and conditions: (a) B_2O_3, tributyl borate, *n*-$C_4H_9NH_2$, EA, 25 °C, 16 h.

Scheme 2. Preparation of Compounds 2a−2e[a]

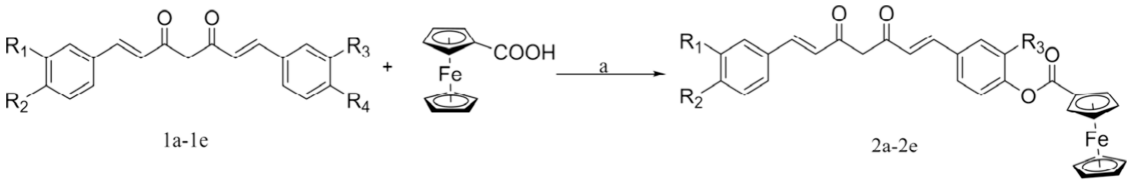

2a: R_1=OCH_3, R_2=OH, R_3=OCH_3
2b: R_1=OCH_3, R_2=OCH_3, R_3=OCH_3
2c: R_1=H, R_2=OH, R_3=H
2d: R_1=OCH_3, R_2=OH, R_3=H
2e: R_1=OCH_3, R_2=OCH_3, R_3=H

[a]Reagents and conditions: (a) EDC, Et_3N, DMAP, DCM, 25 °C, 18 h.

SHP-2.[27] Specifically, DMC prevents SHP-2 from binding to EGFR by downregulating the phosphorylation of SHP-2.

Despite its potential as an SHP-2 target inhibitor, there are few studies on Cur. Consequently, we aim to design and synthesize Cur derivatives as SHP-2 inhibitors. Considering Cur's limitations, such as poor water solubility, rapid metabolism and low bioavailability,[28−30] ferrocene is utilized to modify the structure of Cur due to its chemical stability, lipophilicity, nontoxicity, and redox activity, which enhance its potential value in drug design.[31,32] Chloroquine and tamoxifen have been modified by appending a ferrocene moiety, resulting in both ferrocenyl derivatives demonstrating enhanced biological activities.[33−35] Based on the aforementioned points, we designed and synthesized a series of ferrocenyl-substituted Cur derivatives as SHP-2 target inhibitors, with the design rationale illustrated in Figure 2. Although several ferrocenyl-substituted Cur derivatives have been reported, limited studies have been conducted on their biological activities.[36] Therefore, we synthesized additional derivatives and conducted in-depth pharmacological investigations.

2. RESULTS AND DISCUSSION

2.1. Chemistry. The synthetic route for Cur derivatives **1a−1m** is illustrated in Scheme 1. These derivatives are obtained through the reaction of acetylacetone (**1**) with various benzaldehyde derivatives at room temperature with moderate to high yields. Characterization is performed using ^{1}H NMR, FT-IR, and HRMS.

The structures of derivatives **1a−1m** were confirmed through analytical and spectral data. The ^{1}H NMR analysis revealed peaks between 5.4 and 7.8 ppm for compounds **1a−1e**, confirming the successful synthesis of the diaryl heptadienedione core structure. The ^{1}H NMR spectrum exhibited singlet signals around δ 3.9 ppm, corresponding to the $-OCH_3$ protons.

The determination of the structures of products **1g−1m** required meticulous analysis of their spectral data. The ^{1}H NMR spectrum of compound **1g** displayed a singlet signal for 12 protons corresponding to the methyl group at 2.29 ppm. The ^{1}H NMR spectrum of compound **1h** showed 12 protons in the alicyclic region at 1.26 and 1.27 ppm, while compound **1i** exhibited a singlet signal for 18 protons at 1.34 ppm,

https://doi.org/10.1021/acsomega.4c10629
ACS Omega 2024, 9, 51701−51718

corresponding to the $-CH(CH_3)_2$ and $-C(CH_3)_3$ groups, respectively. The ^{1}H NMR spectrum of compound **1j** showed 15 protons at 5.86−7.70 ppm. The ^{1}H NMR spectra of compound **1k**−**1m** each displayed 13 protons in the range of 5.80 to 7.80 ppm.

Ferrocenyl-substituted Cur formic ester derivatives (**2a**−**2e**) are initially prepared via a one-pot reaction of Fc-COOH (**2**, ferrocenecarboxylic acid) and Cur derivatives (**1a**−**1e**) in the presence of EDC and DMAP under mild conditions (Scheme 2). All derivatives are characterized by ^{1}H NMR, ^{13}C NMR, FT-IR, and HRMS.

The specific structures of derivatives **2a**−**2e** were confirmed through an analysis of spectral data. The ^{1}H NMR spectra of compounds **2a**−**2e** displayed multiple signals for 9 protons between 4 and 5 ppm, corresponding to the ferrocene group. In comparison to their precursor compounds (**1a**−**1e**), all derivatives lacked a proton from the hydroxyl group.

Ferrocenyl-substituted Cur derivatives (**3a**−**3m**) were synthesized via a Knoevenagel reaction between FcCHO (**3**, ferrocene carboxaldehyde) and Cur derivatives (**1a**−**1m**) in DMF in the presence of piperidine at ambient temperature (Scheme 3). All compounds were isolated and purified as powder by column chromatography and subsequently characterized using ^{1}H NMR, ^{13}C NMR, FT-IR and HRMS.

Scheme 3. Preparation of Compounds 3a−3m[a]

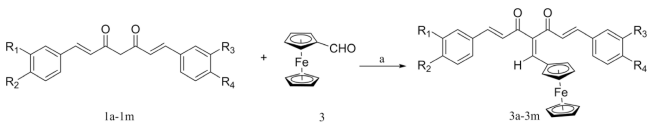

3a: R_1=OCH_3, R_2=OH, R_3=OCH_3, R_4=OH
3b: R_1=OCH_3, R_2=OCH_3, R_3=OCH_3, R_4=OH
3c: R_1=H, R_2=OH, R_3=H, R_4=OH
3d: R_1=OCH_3, R_2=OH, R_3=H, R_4=OH
3e: R_1=OCH_3, R_2=OCH_3, R_3=H, R_4=OH
3f: R_1=OCH_3, R_2=OCH_3, R_3=OCH_3, R_4=OCH_3
3g: R_1=CH_3, R_2=CH_3, R_3=CH_3, R_4=CH_3
3h: R_1=H, R_2=$CH(CH_3)_2$, R_3=H, R_4=$CH(CH_3)_2$
3i: R_1=H, R_2=$C(CH_3)_3$, R_3=H, R_4=$C(CH_3)_3$
3j: R_1=H, R_2=H, R_3=H, R_4=H
3k: R_1=H, R_2=Br, R_3=H, R_4=Br
3l: R_1=H, R_2=Cl, R_3=H, R_4=Cl
3m: R_1=H, R_2=F, R_3=H, R_4=F

[a]Reagents and conditions: (a) Piperidine, DMF, 25 °C, 48 h.

The ^{1}H NMR analysis indicated that, compared to the precursor compounds (**1a**−**1m**), the active methylene proton signal for compounds **3a**−**3m** disappeared at approximately 5.80 ppm. Similar to compounds **2a**−**2e**, compounds **3a**−**3m** exhibited multiple signals for 9 protons of ferrocene between 4 and 5 ppm.

2.2. Biological Evaluation. *2.2.1. In Vitro Antiproliferative Activities.* All ferrocenyl-substituted Cur derivatives (**2a**−**2e** and **3a**−**3m**) were tested using the MTT assay to evaluate their antiproliferative effects against various CRC cell lines, including human CRC cell lines RKO and SW480 and the mouse CRC cell line CT26. The IC_{50} values are summarized in Table 1. These cell lines were selected because SHP-2, a protein-tyrosine phosphatase (PTP), is widely present in the cytoplasm and is reportedly highly expressed in CRC.[37]

The effects of compounds **2a**−**2e** and **3a**−**3m**, along with Cur as a control group, on the human CRC cell line RKO at different concentrations are presented in Figure 3A. The results indicated that the inhibitory activity of most compounds against RKO cells was dose-dependent. At administered concentrations of 10 and 20 μM, most

Table 1. Antiproliferative Effects of the Synthesized Molecules against the RKO Cell Line

compound	IC_{50}	compound	IC_{50}	compound	IC_{50}
2a	23.21	**3b**	5.66	**3h**	107.5
2b	64.27	**3c**	7.66	**3i**	
2c	46.55	**3d**	11.91	**3j**	5.64
2d	11.05	**3e**	7.29	**3k**	17.20
2e	149.40	**3f**	5.72	**3l**	10.47
3a	12.51	**3g**	59.13	**3m**	5.08

compounds exhibited significant activity in inhibiting the proliferation of RKO cells compared to Cur. However, at concentrations of 40 and 80 μM, there was no significant difference between all compounds and the Cur control group ($^*p > 0.05$).

Overall, compounds **2a**−**2e** exhibited weaker inhibitory effects on the proliferation of RKO cells compared to derivatives **3a**−**3m**; however, compounds **2a** and **2d** demonstrated significant activity, particularly **2d**, which had an IC_{50} value of 11.05 μM. This suggests that the ester derivatives formed from the reaction of ferrocene with the phenolic hydroxyl group of Cur possess significant potential to inhibit CRC cell proliferation and warrant further investigation. Furthermore, compounds with methoxy substituents (**3a**−**3f**; IC_{50} = 5.51, 5.66, 7.66, 11.91, 7.29, and 5.72 μM, respectively) and those with halogen substituents **3k**−**3m** (IC_{50} = 17.20, 10.47, and 5.08 μM, respectively) exhibited better inhibition of RKO cell proliferation compared to the alkyl-substituted compounds (**3g**−**3i**; IC_{50} > 20 μM). This outcome could be attributed to the electronic effects and steric hindrance. Regarding compounds **3g**−**3i**, there was no significant difference in their ability to inhibit RKO cell proliferation compared to Cur. Excitingly, compound **3j** displayed unexpectedly high activity against RKO cell proliferation, with an IC_{50} value of 5.64 μM. This may be due to the absence of a substituent on the benzene ring, which reduced the impact of steric hindrance on drug activity.

Based on the findings, compounds **3a**−**3c** and **3e**−**3f** were selected for further medicinal efficacy investigations. The effects of compounds **3a**−**3c** and **3e**−**3f** on the human CRC cell line SW480 and the mouse CRC cell line CT26 at a concentration of 10 μM are presented in Figure 3B. Compound CVB-D (12 μM) served as the positive control.

The results indicated that in the SW480 cell line, the CVB-D group exhibited significant differences compared to the control group ($^*p < 0.05$), while the **3b** and **3f** groups demonstrated even more significant differences ($^{**}p < 0.01$ and $^{***}p < 0.001$). This suggests that the inhibition of SW480 cells by compounds **3b** and **3f** was markedly superior to that of the CVB-D group. In the CT26 cell line, compounds **3b** and **3f** displayed significant differences compared to the control group, with values of $^*p < 0.05$ and $^{***}p < 0.001$, respectively. Compared to the CVB-D group, compound **3f** still exhibited a significant difference ($^{\#}p < 0.05$), while **3b** showed no significant difference. These findings indicate that **3f** exhibited stronger anti-CRC activity compared to both the control group and the positive drug CVB-D. In summary, **3f** is an effective compound against CRC and needs further investigation.

2.2.2. Optimal Inhibition Concentration of Compound 3f. CRC cell lines SW480 and CT26 were treated with **3f** at various concentrations (0, 1, 2, 3, 4, 5, 6, 7, and 8 μM) to determine the optimal inhibitory concentration (Figure 4). In

https://doi.org/10.1021/acsomega.4c10629
ACS Omega 2024, 9, 51701−51718

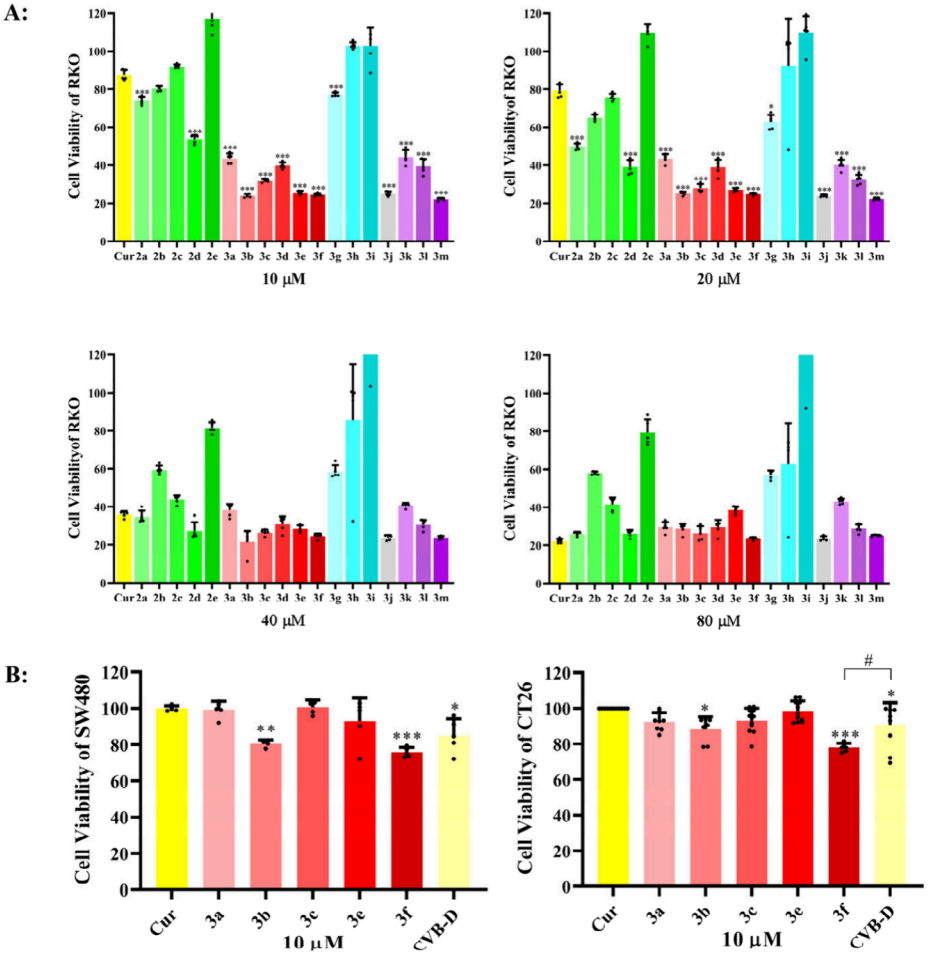

Figure 3. Effect of compounds on the proliferative capacity of RKO, SW480, and CT26 cells. (A) Effect of compounds **2a**−**2e** and **3a**−**3m** on the proliferative capacity of RKO cells. (B) Effect of compounds **3a**−**3c** and **3e**−**3f** on the proliferative capacity of SW480 and CT26 cells. $^{*}p < 0.05$, $^{**}p < 0.01$, $^{***}p < 0.001$ vs Cur, and $^{\#}p < 0.05$ vs CVB-D.

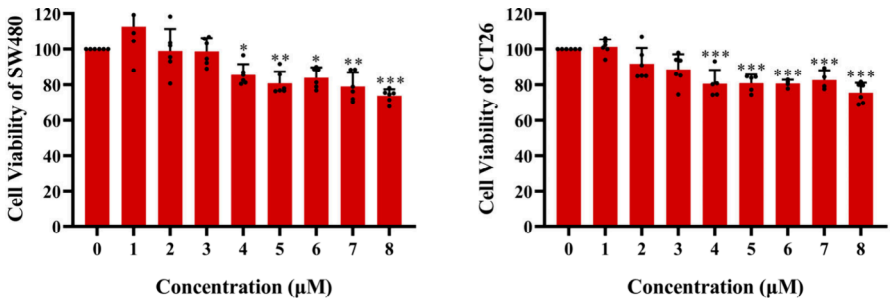

Figure 4. Effect of compound **3f** (0−8 μM) on the viability of SW480 and CT26 cell lines. $^{*}p < 0.05$, $^{**}p < 0.01$, $^{***}p < 0.001$ vs control.

the SW480 cell line, **3f** began to demonstrate a significant inhibition effect at a concentration of 4 μM compared to the control group ($^{*}p < 0.05$). As the concentration of **3f** increased, the inhibition effect was progressively enhanced. When the concentration reached 8 μM, **3f** exhibited a significant difference ($^{***}p < 0.001$) and showed the strongest inhibitory activity against SW480 cells, with an IC_{50} value of 3.71 μM. Similarly, in the CT26 cell line, **3f** (IC_{50} = 1.42 μM) demonstrated an inhibitory effect at a concentration of 3 μM, and at concentrations of 4−8 μM there was a significant difference ($^{***}p < 0.001$) compared to the control group. The optimal inhibitory concentration was also noted at 8 μM. These results indicate that **3f** exhibits a strong inhibitory effect and has potential as an anti-CRC drug. Therefore, to further investigate the anticancer mechanism of **3f**, the concentration was set at 8 μM.

2.2.3. Cytotoxicity against Normal Cell Lines and Selectivity Index (SI). The effects of Cur and **3f** at various concentrations (0, 5, 10, 20, 40, and 80 μM) on the human normal colon epithelial cell line NCM460 are presented in Figure 5A. After treatment with **3f** (IC_{50} = 929 μM), the viability of NCM460 cells remained above 87% at all concentrations, demonstrating lower toxicity than Cur, which has an IC_{50} value of 431 μM. According to the USP toxicity classification, **3f** was determined to be low toxic/nontoxic to normal colon epithelial cells. In other words, compound **3f**

https://doi.org/10.1021/acsomega.4c10629
ACS Omega 2024, 9, 51701−51718

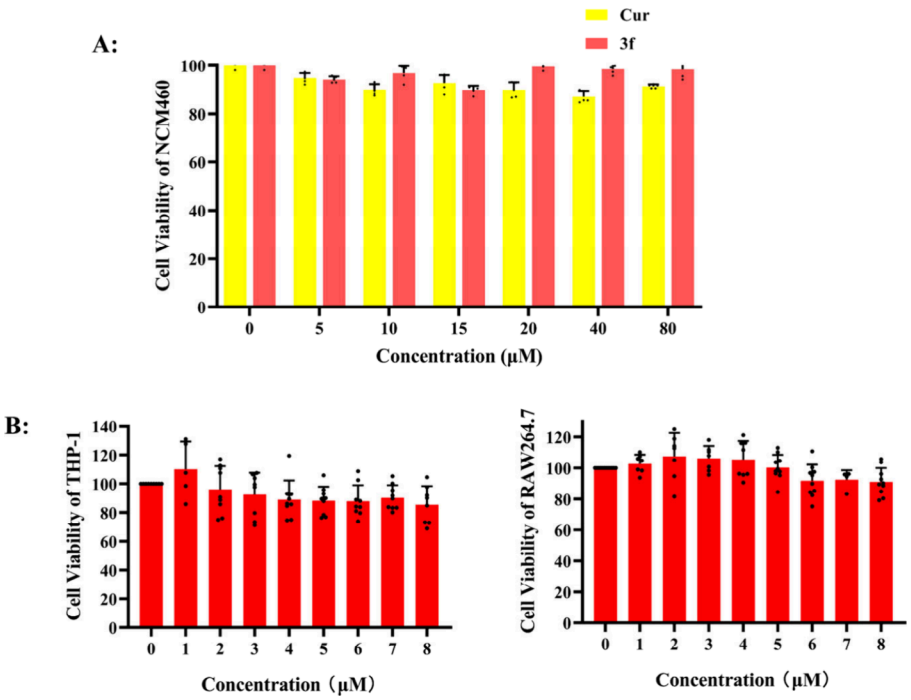

Figure 5. Effects of compound **3f** on the cell viability of NCM460, THP-1, and RAW264.7(B) cells. (A) Effects of Cur and **3f** (0, 5, 10, 20, 40, and 80 μM) on the viability of the NCM460 cell line. (B) Effect of compound **3f** (0−8 μM) on the viability of THP-1and RAW264.7 cell lines.

exhibits high safety and good biocompatibility with normal colon cells.

The selectivity index (SI) of compound **3f** was calculated as the ratio of the IC_{50} values for normal cells to those for CRC cells. The results indicated that the SI of compound **3f** for the three CRC cell lines RKO, SW480, and CT26 were 162, 250, and 654, respectively. Based on all the experiments conducted, we conclude that compound **3f** effectively inhibits CRC cells while exhibiting no or low toxicity toward normal colon cells.

*2.2.4. Effect ofCcompound **3f** on the THP-1 Cell Line and RAW264.7 Cells.* Chronic inflammation is a significant factor in tumorigenesis. Therefore, it is essential to investigate the effect of compound **3f** on immune cells in the TME. The RAW264.7 cell line is one of the most commonly used models for studying inflammatory cells. THP-1, a human monocytic leukemia cell line, is widely utilized to study macrophage-related mechanisms and signaling pathways.

The cytotoxicity results of **3f** at concentrations ranging from 0 to 8 μM on the THP-1 and RAW264.7 cell lines are presented in Figure 5B. The results indicate that the cell viability of THP-1 and RAW264.7 cells treated with **3f** remained close to 100% at all concentrations, with no significant difference compared with the control group. This suggests that compound **3f** does not affect the THP-1 and RAW264.7 cell lines.

*2.2.5. Effect of Compound **3f** on Cell Cycle-Related and Mitophagy-Related Proteins in CT26 and SW480 Cell Lines.* This experiment investigated the effect of **3f** on cell cycle-related and mitophagy-related proteins in SW480 and CT26 cell lines at concentrations of 0 (control group) and 8 μM. The results of the Western blot analysis are presented in Figure 6.

In the SW480 cell line (Figure 6A), compared to the control group, **3f** reduced the expression of Cyclin-D1 protein, achieving an inhibition rate of 19%, with the results being statistically different (***p < 0.001). Furthermore, **3f** significantly increased the expression of p27 protein (***p < 0.001), indicating that **3f** could induce cell cycle arrest and inhibit the proliferation of SW480 cells by regulating p27 expression. In addition, treatment with **3f** significantly up-regulated PINK1 and Parkin proteins (***p < 0.001), thereby activating mitophagy and inhibiting tumor occurrence and progression. In the CT26 cell line (Figure 6B), **3f** exhibited a stronger inhibitory effect on Cyclin-D1 protein compared to SW480 and was more effective in regulating the overexpression of Cyclin-D1 in tumor cells, thereby reducing tumor cell proliferation. Similarly, the expression of the other three proteins (p27, PINK1, Parkin) would also be significantly increased after the treatment of **3f**, but the effect was not as good as that in the SW480 cell line.

The results indicate that **3f** inhibits tumor proliferation by inducing cell cycle arrest and promoting mitophagy. This further demonstrates that **3f** has the potential to serve as a colorectal cancer inhibitor capable of influencing tumor development through multiple pathways.

2.2.6. In Vitro SHP-2, CDK1, PI3K, and Akt Inhibitory Activity. The results of the effect of compound **3f** on the expression of SHP-2, CDK1, PI3K, and Akt in the SW480 and CT26 cell lines are presented in Figure 7.

As shown in Figure 7A and B, compound **3f** exhibited the highest inhibitory activity against the SHP-2 target in the SW480 cell line, with an inhibition rate reaching as high as 76%. However, in the CT26 cell line, **3f** inhibited the SHP-2 target by only 24%. Both results were significantly different from those of the control group (***p < 0.001). These results indicate that compound **3f** exerts a strong inhibitory effect on the SHP-2 target.

CDK1 is commonly found in tumor cells as a cell cycle-related target protein.[38] When phosphorylated, CDK1 promotes the cell cycle progression. Given that SHP-2 is a member of the PTP family, we speculated that there may be a connection between the two targets, SHP-2 and CDK1. The presence of SHP-2 may lead to the phosphorylation of CDK1,

https://doi.org/10.1021/acsomega.4c10629
ACS Omega 2024, 9, 51701−51718

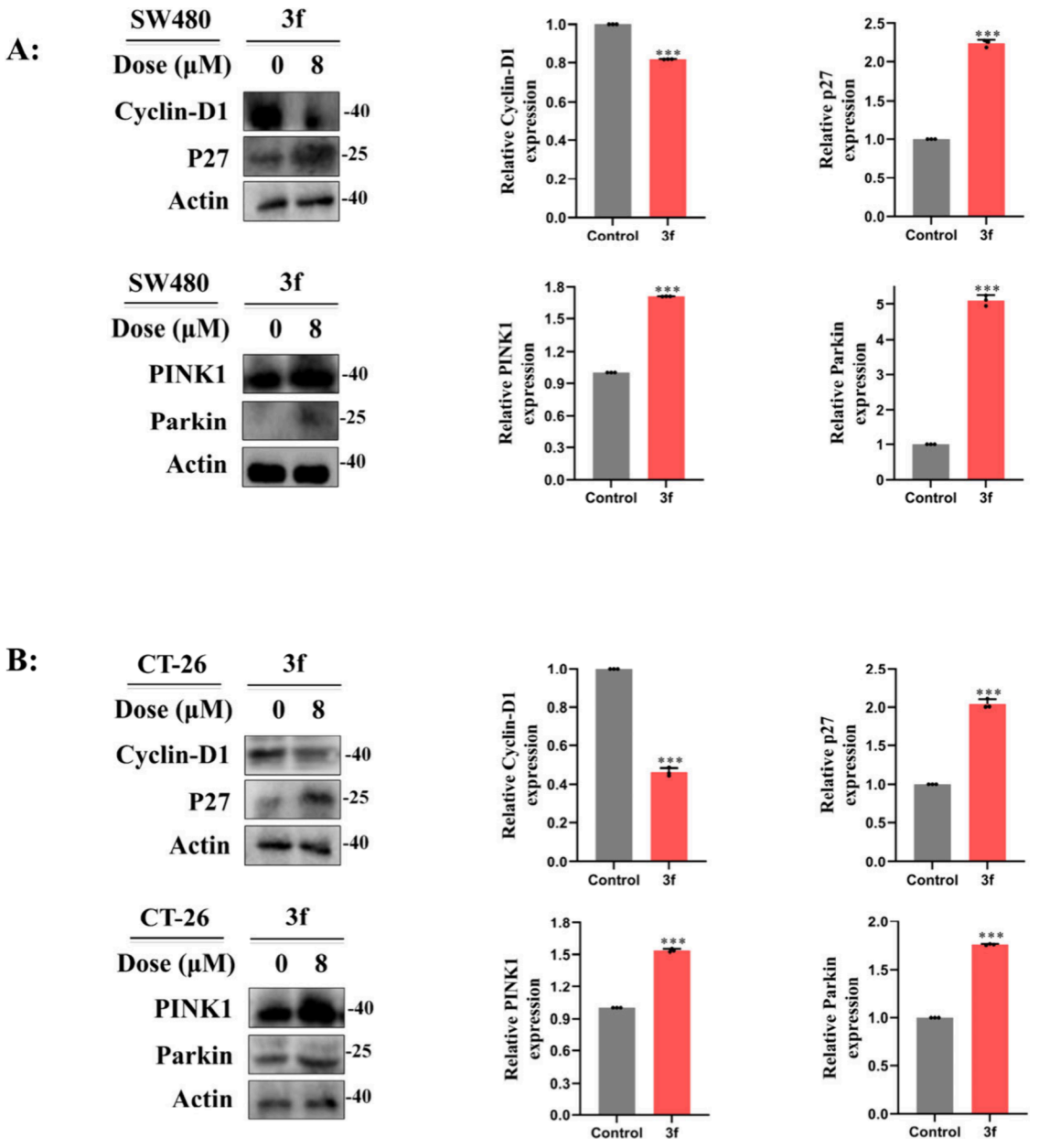

Figure 6. Effect of **3f** on cell cycle- and mitophagy-related protein expression in SW480 and CT26 cells. (A) Effect of **3f** (0 and 8 μM) on the expression of cell cycle-related and mitophagy-related proteins in the SW480 cell line. (B) Effect of **3f** (0 and 8 μM) on the expression of cell cycle-related and mitochondrial autophagy marker proteins in the CT26 cell line. ***$p < 0.001$ vs control.

resulting in tumor cell proliferation. The inhibition results of **3f** on the CDK1 target are presented in Figure 7A and B. The CDK1 inhibition rates in the SW480 and CT26 cell lines were 18% and 20%, respectively. Both results were significantly different from those of the control group (***$p < 0.001$). These results indicate that **3f** significantly inhibits the CDK1 target, supporting its role as a dual-target inhibitor.

Based on the previous experiments, the effect of **3f** on the SHP-2-related PI3K/Akt pathway was further investigated. The PI3K-Akt pathway plays an crucial role in the occurrence and development of various of tumors,[39] making its inhibition a common anticancer strategy. In the SW480 cell line (Figure 7A), the expression of PI3K and Akt proteins was significantly inhibited (***$p < 0.001$) at a concentration of 8 μM of **3f**. The inhibition rates of **3f** on PI3K and Akt were 46% and 48%, respectively. Therefore, **3f** inhibited the PI3K-Akt pathway in SW480 cells, thereby reducing the level of cell proliferation. In the CT26 cell line (Figure 7B), the inhibition rates of **3f** on the expression of PI3K and Akt proteins were 15% and 50%, respectively, and these results showed significant differences (***$p < 0.001$). In summary, compound **3f** inhibited the PI3K-Akt pathway. Despite the suppression of SHP-2 protein expression, SHP-2 continued to inhibit the PI3K-Akt pathway.

*2.2.7. Effect of Compound **3f** in the TME.* The antitumor activity of drugs cannot be assessed solely in tumor cells, as tumor cells can remodel their environment to increase tumor growth.[40] These drugs not only exert anticancer effects by directly killing tumor cells but also inhibit macrophage cancer-promoting phenotypes by affecting immune cells in the TME. Therefore, investigating the effect of compound **3f** in the TME is essential. In this study, SW480 and CT26 cells were independently cocultured with the THP-1 and RAW264.7 cell

https://doi.org/10.1021/acsomega.4c10629
ACS Omega 2024, 9, 51701−51718

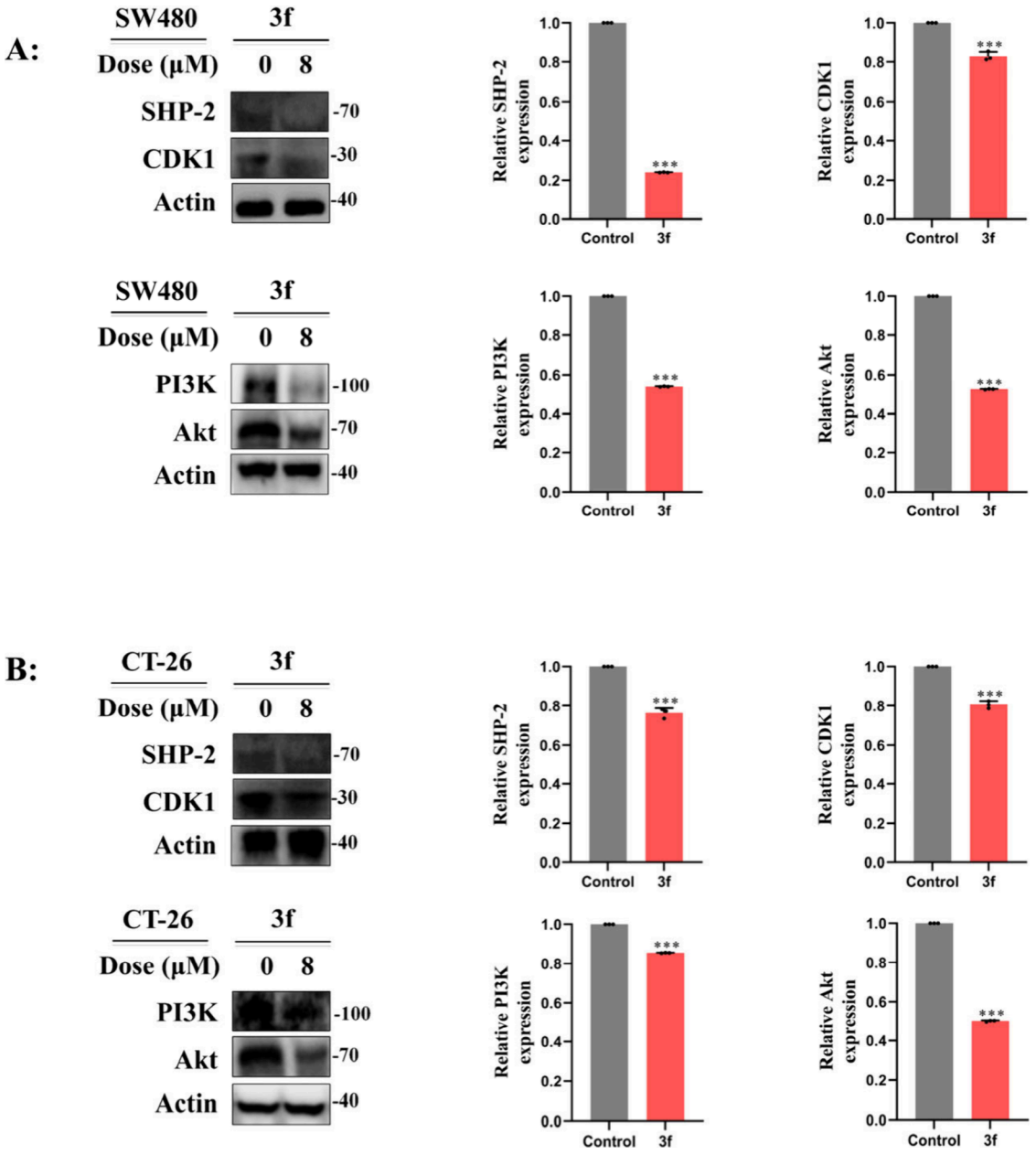

Figure 7. Effect of **3f** on the protein expression of SHP-2, CDK1, PI3K, and Akt in SW480 and CT26 cells. (A) Effect of **3f** (0 and 8 μM) on SHP-2, CDK1, PI3K, and Akt protein expression in the SW480 cell line. (B) Effect of **3f** (0 and 8 μM) on SHP-2, CDK1, PI3K, and Akt protein expression in the CT26 cell line. ***$p < 0.001$ vs control.

lines to induce macrophages to differentiate into cancer-promoting immune cells, after which the effect of **3f** on these cells was investigated.

M2-TAMs secrete immunosuppressive cytokines that inhibit immune responses and create a TME that promotes cancer-promoting phenotype. Therefore, the anti-inflammatory cytokines (TGF-β, IL-10, and Arg-1) in the TME were selected for Western blot analysis. The results are analyzed in Figure 8.

Compared to the control group, the expression levels of cytokines (TGF-β, IL-10, and Arg-1) in the TME were significantly increased after coculturing, with results being statistically significant (***$p < 0.001$). Following treatment with **3f**, the expression levels of cytokines in the TME were significantly reduced, and the results were again statistically significant ($^{\#\#\#}p < 0.001$). These results indicate that **3f** not only directly inhibits the activity of SW480 and CT26 cell lines but also impedes tumor growth by reducing the level of expression of certain inhibitory cytokines in the TME.

The SHP-2 target in both groups was assessed by using **3f**, and the results are presented in Figure 7. The results indicate that compound **3f** significantly reduces the expression level of SHP-2 in the TME of both groups. The results were significantly different from those of the control group (***$p < 0.001$). Similarly, the inhibition rate of **3f** on the SHP-2 target in human TME (65%) was greater than that in mouse TME (32%). These findings support **3f** as an SHP-2 target inhibitor.

Next, the PI3K-Akt pathways in the TAMs were also investigated. In both coculture systems (Figure 8), **3f** reduced the expression levels of PI3K and Akt proteins, showing significant differences compared to the control group (***$p <$

https://doi.org/10.1021/acsomega.4c10629
ACS Omega 2024, 9, 51701−51718

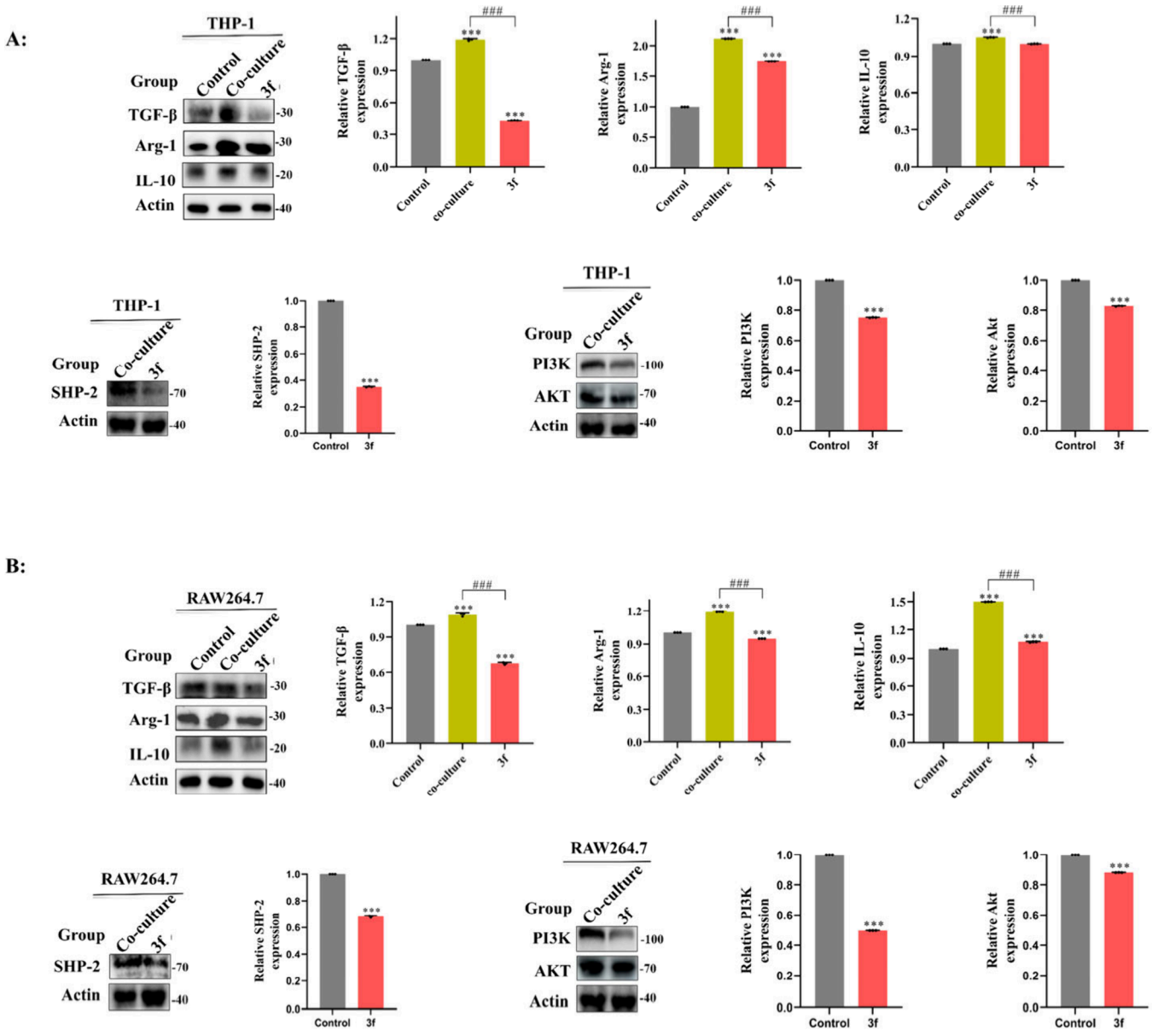

Figure 8. Effect of compound **3f** on cytokine, SHP-2, PI3K, and Akt expression. (A) Effect of **3f** on cytokine, SHP-2, PI3K, and Akt expression in the THP-1 cell line (coculture: SW480 cells are cocultured with THP-1 cells). (B) Effect of **3f** on cytokine, SHP-2, PI3K, and Akt expression in RAW264.7 cell line (coculture: CT26 cells are cocultured with RAW264.7 cells). ***$p < 0.001$ vs control; ###$p < 0.001$ vs coculture.

0.001). The decrease in PI3K expression indicates that M2-TAMs are inhibited, resulting in tumor cells losing their ability to suppress PD-1 and other antibodies in immunotherapy.

*2.2.8. Effect of Compound **3f** on Chemokines.* Chemokines are cytokines that mediate the transport of immune cells. In cancer, they primarily facilitate the migration of immune cells into tumors, contributing to the immune characteristics of the cancer-promoting TME.[41] Therefore, this study investigates the inhibition effects of the drug on macrophage aggregation mediated by relevant chemokines, including chemokine receptors (CCR1, CCR2, CCR5, CCR7, CCR8, and CCR9), CC chemokine subfamilies (CCL2, CCL3, CCL4, CCL5, and CCL7), and CXC chemokine subfamilies (CXCL1, CXCL2, CXCL3, CXCL5, and CXCL10).

The effects of compound **3f** on chemokine *m*RNA levels in the human TME (Figure 9A) and in the mouse TME (Figure 9B) are presented as follows. Following administration, compound **3f** significantly reduced the *m*RNA levels of CCR chemokine receptors and inhibited macrophage aggregation, demonstrating its antitumor activity. In addition, the results indicated that **3f** was able to inhibit CCL and CXCL subfamilies. In summary, compound **3f** exerts an inhibitory effect on the occurrence and development of the TME, strongly suggesting that **3f** could be a potential antitumor drug for the treatment of CRC.

2.3. Docking Study. Molecular docking was conducted by using AutoDockTools ver. 1.5.6. This software was employed to predict the binding mode of compound **3f** to receptors of CRC proteins. Compound **3f** was docked against acetaldehyde dehydrogenase 1 (ALDH1, PDB ID: 5ABM). The crystal structure of ALDH1 was prepared for docking. Chains B, C, and D were removed, while chain A was hydrogenated and dehydrated. Missing amino acid residues were added for structural optimization. The active pocket was designed to

https://doi.org/10.1021/acsomega.4c10629
ACS Omega 2024, 9, 51701−51718

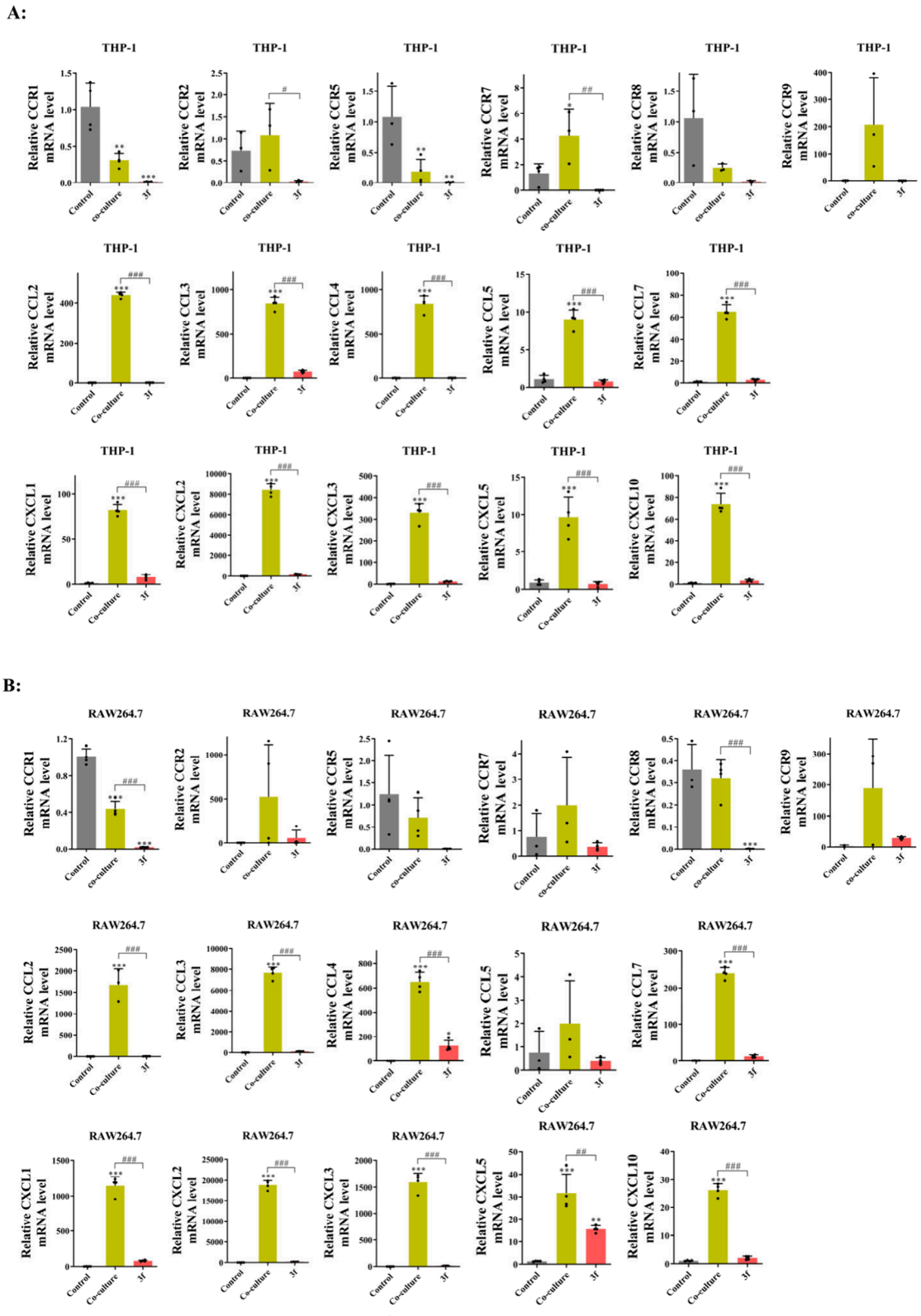

Figure 9. Effects of compound **3f** on the *m*RNA level of chemokine in THP-1 cells and the RAW264.7 cell line. (A) Effect of **3f** on the *m*RNA level of chemokine in the THP-1 cell line (coculture: SW480 cells are cocultured with THP-1 cells). (B) Effect of **3f** on the *m*RNA level of chemokine in the RAW264.7 cell line (coculture: CT26 cells are cocultured with RAW264.7 cells). $^{*}p < 0.05$, $^{**}p < 0.01$, $^{***}p < 0.001$ vs control; $^{\#\#}p < 0.01$, $^{\#\#\#}p < 0.001$ vs coculture.

focus on active site Cys 302 of the receptor protein ALDH1. The binding energy values of **3f** to ALDH1 is −10.2 kcal/mol, less than that of Cur (−8.4 kcal/mol) with ALDH1, indicating that compound **3f** had more effective anti-CRC activity. The two methoxy groups on the benzene ring formed hydrogen bonds with ALA 461 and THR 128, with bond distances of 3.0

https://doi.org/10.1021/acsomega.4c10629
ACS Omega 2024, 9, 51701−51718

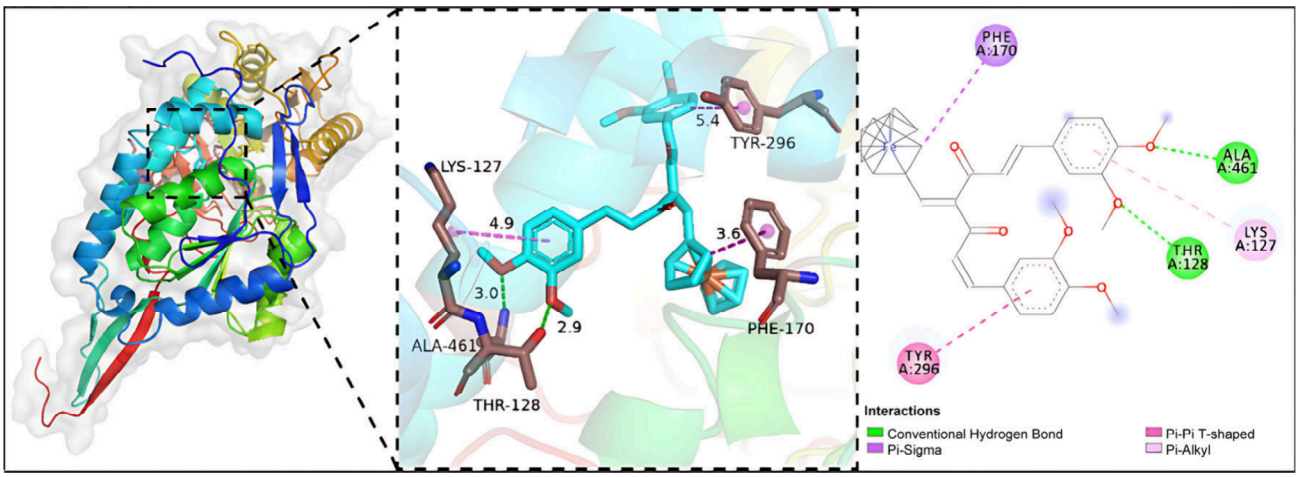

Figure 10. Results of docking **3f** with ALDH1.

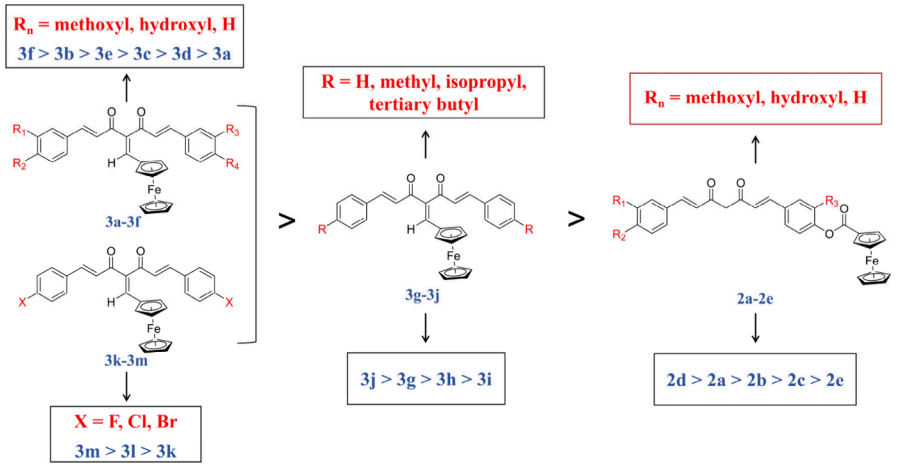

Figure 11. SAR of the ferrocenyl-substituted Cur derivatives as SHP-2 inhibitors.

and 2.9 Å, respectively. The benzene ring exhibited a $\pi-\pi$ stacking interaction with TYR 296 with a bond distance of 5.4 Å and a hydrophobic interaction with LYS 127 with a bond distance of 4.9 Å. Additionally, ferrocene may exhibit an $\pi-\pi$ stacking interaction with PHE 170 (Figure 10).

Compound **3f** is situated in the active center of the ALDH1 protein, forming a stable hydrophobic interaction with the hydrophobic region of the active pocket. It effectively interacts with multiple hydrogen bond acceptors and oxygen bond donors to form a complex with better binding energy and good stability; thereby, it inhibits enzyme activity.

2.4. Structure−Activity Relationship (SAR). The results of the SAR study of ferrocenyl-substituted Cur derivatives are illustrated in Figure 11. Results from MTT assay, Western blot assay, and molecular docking indicate that, in general, the anti-CRC effects of compounds **3a−3m** are superior to those of **2a−2e**. Furthermore, among compounds **3a−3m**, compound **3f** exhibits the highest anticancer activity.

Compound **3f**, with an electron-donating substituent ($-OCH_3$), demonstrates excellent anti-CRC activity, which can be attributed to the formation of hydrogen bonds between the methoxy group and CRC cell-related protein receptors, as observed in the molecular docking analysis. These hydrogen bonds facilitate the binding of **3f** to proteins, thereby enhancing its activity in inhibiting the proliferation of CRC cells. Moreover, the position and numbers of methoxy groups strongly influence the anticancer properties of Cur,[42−45] as reported. For example, in this study, among the methoxy-substituted compounds **3b**, **3d**, **3e**, and **3f**, **3f** with four methoxy groups exhibits the highest anticancer activity, followed by **3b** with three methoxy groups and **3e** with two methoxy groups, with **3d** with only one methoxy group being least active.

Additionally, compounds **3g−3i**, which are also substituted with electron-donating groups (methyl, isopropyl, and *tert*-butyl, respectively), display poor anti-CRC activity. One reason is that alkyl groups cannot form hydrogen bonds or other strong interactions with proteins such as the methoxy group, leading to a decreased binding ability of these compounds with proteins. Moreover, from the perspective of steric hindrance, isopropyl and *tert*-butyl substituents are large and more sterically hindered, which may impede the binding of compounds to targets in certain cases, thereby reducing their biological activity. In contrast, the steric effects of the methyl and methoxy groups are smaller, resulting in relatively improved anticancer activity. Notably, compound **3j**, which contains no substituent on the benzene ring, demonstrates better anti-CRC activity, likely attributed to reduced steric hindrance. Therefore, based on the analysis of steric hindrance, the larger the steric hindrance, the weaker the anticancer activity.

https://doi.org/10.1021/acsomega.4c10629
ACS Omega 2024, 9, 51701−51718

3. CONCLUSIONS

Eighteen ferrocenyl-substituted Cur derivatives were synthesized as inhibitors of SHP-2. The antiproliferative effects of the synthesized compounds against RKO, SW480, and CT26 cell lines revealed that compound **3f** exhibited the highest activity with IC_{50} values of 5.72, 3.71, and 1.42 μM, respectively. SAR research suggested that methoxy was more advantageous as a pharmacophore than other substituents. Additionally, groups with small steric hindrance were more beneficial than those with a large steric hindrance. The optimized inhibitory concentration of **3f** was determined to be 8 μM. Compound **3f** demonstrated low toxicity/nontoxicity toward NCM460, THP-1, and RAW264.7 cell lines. Western blot analysis indicated that **3f** significantly reduced the expression levels of SHP-2, PI3K, and Akt in both the SW480 and CT26 cell lines, as well as in the TME. Compound **3f** reduced the expression levels of cytokines (Arg-1, TGF-β, and IL-10) and *m*RNA levels of chemokines in the TME. Compound **3f** promoted cell cycle arrest and mitophagy in SW480 and CT26 cell lines by increasing the expression level of p27, PINK1, and Parkin proteins while decreasing the expression level of CDK1 and Cyclin-D1 proteins. To rationalize the results of the biological testing, the synthesized compounds were docked against ALDH1 (PDB ID: 5ABM) to demonstrate favorable binding modes with CRC-related proteins.

4. METHODS

4.1. Chemistry. All reagents and solvents were obtained commercially from Maclean's Reagents Ltd. and used without purification. Thin layer chromatography (TLC) was performed on silica gel GF254. Column chromatography was performed on silica gel 200−300. All ^{1}H NMR and ^{13}C NMR experiments were carried out at room temperature on Bruker 400 MHz NMR spectrometers. High-resolution liquid-mass spectrometry was performed with a Xevo G2S-Q-TOF spectrometer. A UV-2401PC spectrometer was used for UV−visible spectroscopy, and infrared analysis was performed using FT-IR (Fourier transform infrared spectroscopy). Melting point measurements were performed using X-4A microscopic spectrometers.

*4.1.1. General Procedure for the Synthesis of Cur Derivatives (**1a**−**1m**).* To a solution of B_2O_3 (0.98 g, 14.0 mmol) in anhydrous EtOAc (200 mL) were added acetylacetone (2 mL) and tributylborate (10.72 mL, 40 mmol) were added dropwise, and the mixture was stirred under N_2 for 0.5 h. Then, the corresponding benzaldehydes were added and stirred for another 0.5 h, and *n*-butylamine (2 mL) was added afterward and stirred for 16 h in the absence of light. The whole process was monitored for completion by TLC. After 16 h, AcOH (8 mL) was added, and the mixture continued to stir for 10 min. The reaction mixture was quenched with saturated NaCl solution (30 mL) and extracted with EtOAc (3 × 30 mL). Then the organic phase was combined, dried over anhydrous $MgSO_4$, and concentrated *in vacuo*.

*(1E,4Z,6E)-5-Hydroxy-1,7-bis(4-hydroxy-3-methoxyphenyl)hepta-1,4,6-trien-3-one (**1a**, Cur).* Following the general procedure for the synthesis of Cur derivativess, the corresponding benzaldehyde is vanillin (6.09 g, 40 mmol), and compound **1a** (30%) was afforded after purification by recrystallization (EtOH/H_2O) as a yellow solid; mp 181−183 °C. ^{1}H NMR (400 MHz, DMSO-d_6) δ 7.55 (d, J = 15.8 Hz, 2H), 7.33 (s, 2H), 7.16 (d, J = 8.3 Hz, 2H), 6.83 (d, J = 8.1 Hz, 2H), 6.76 (d, J = 15.9 Hz, 2H), 6.07 (s, 1H), 3.84 (s, 6H); IR data ν (cm^{-1}) 3464 (−OH), 1627 (—C═O), 1512, 1414 (Ar), 1273, 1020 (Ar−C−O−C), 1220 (Ar−C−O). The ^{1}H NMR data of compound **1a** are consistent with the reported literature values.[45]

*(1E,4Z,6E)-7-(3,4-Dimethoxyphenyl)-5-hydroxy-1-(4-hydroxy-3-methoxyphenyl)hepta-1,4,6-trien-3-one (**1b**).* Following the general procedure for the synthesis of Cur derivatives, the corresponding benzaldehydes are vanillin (3.05 g, 20 mmol) and veratraldehyde (3.32 g, 20 mmol), and compound **1b** (3.0%) was afforded after purification by column chromatography (petroleum ether/EtOAc, 2:1) as an orange solid; mp 70−73 °C. ^{1}H NMR (400 MHz, $CDCl_3$) δ 7.62 (dd, J = 15.8, 6.8 Hz, 2H), 7.16 (t, J = 8.6 Hz, 2H), 7.09 (d, J = 12.0 Hz, 2H), 6.96 (d, J = 8.2 Hz, 1H), 6.91 (d, J = 8.3 Hz, 1H), 6.51 (dd, J = 15.8, 7.9 Hz, 2H), 5.91−5.80 (m, 2H), 3.97 (s, 3H), 3.96 (s, 3H), 3.95 (s, 3H); IR data ν (cm^{-1}) 3414 (−OH), 2826 (−OCH_3), 1628 (—C═O), 1581, 1513, 1457 (Ar), 1267, 1022 (Ar−C−O−C); HRMS (ESI) m/z [M − H]$^-$ calcd. for $[C_{22}H_{21}O_6]^-$ 381.1416, found 381.1338.

*(1E,4Z,6E)-5-Hydroxy-1,7-bis(4-hydroxyphenyl)hepta-1,4,6-trien-3-one (**1c**).* Following the general procedure for the synthesis of Cur derivatives, the corresponding benzaldehyde is *p*-hydroxybenzaldehyde (4.88 g, 40 mmol), and compound **1c** (39.8%) was afforded after purification by recrystallization (EtOH/H_2O) as an orange red solid; mp 220−221 °C. ^{1}H NMR (400 MHz, $CDCl_3$) δ 7.58−7.56 (m, 4H), 7.54 (d, J = 13.8 Hz, 2H), 6.82 (d, J = 8.5 Hz, 4H), 6.69 (d, J = 15.8 Hz, 2H), 6.04 (s, 1H); IR data ν (cm^{-1}) 3244 (−OH), 1627 (—C═O), 1600, 1565, 1510, 1434 (Ar), 1270, 1020 (Ar−C−O−C). The ^{1}H NMR data of compound **1c** are consistent with the reported literature values.[46]

*(1E,4Z,6E)-5-Hydroxy-7-(4-hydroxy-3-methoxyphenyl)-1-(4-hydroxyphenyl)hepta-1,4,6-trien-3-one (**1d**).* Following the general procedure for the synthesis of Cur derivatives, the corresponding benzaldehydes are vanillin (3.05 g, 20 mmol) and *p*-hydroxybenzaldehyde (2.44 g, 20 mmol), and compound **1d** (14.2%) was afforded after purification by column chromatography (petroleum ether/EtOAc, 2:1) as a light red solid; mp 164−169 °C. ^{1}H NMR (400 MHz, $CDCl_3$) δ 7.58 (dd, J = 15.8, 6.2 Hz, 2H), 7.45 (d, J = 8.4 Hz, 2H), 7.12−7.08 (m, 1H), 7.03 (s, 1H), 6.91 (d, J = 8.2 Hz, 1H), 6.84 (d, J = 8.4 Hz, 2H), 6.46 (dd, J = 15.8, 3.9 Hz, 2H), 5.86−5.75 (m, 2H), 3.93 (d, J = 0.9 Hz, 3H); IR data ν (cm^{-1}) 3278 (−OH), 1627 (—C═O), 1580, 1511, 1428 (Ar), 1273, 1026 (Ar−C−O−C). The ^{1}H NMR data of compound **1d** are consistent with the reported literature values.[46]

*(1E,4Z,6E)-7-(3,4-Dimethoxyphenyl)-5-hydroxy-1-(4-hydroxyphenyl)hepta-1,4,6-trien-3-one (**1e**).* Following the general procedure for the synthesis of Cur derivatives, the corresponding benzaldehydes are *p*-hydroxybenzaldehyde (2.44 g, 20 mmol) and veratraldehyde (3.32 g, 20 mmol), and compound **1e** (4.9%) was afforded after purification by column chromatography (petroleum ether/EtOAc, 2:1) as an orange solid; mp 187−200 °C. ^{1}H NMR (400 MHz, $CDCl_3$) δ 7.64 (d, J = 15.7 Hz, 2H), 7.50 (d, J = 8.6 Hz, 2H), 7.17 (d, J = 9.2 Hz, 1H), 7.11 (d, J = 2.0 Hz, 1H), 6.93−6.89 (m, 2H), 6.87 (s, 2H), 6.52 (dd, J = 15.8, 3.0 Hz, 2H), 5.83 (s, 1H), 3.96 (s, 3H), 3.95 (s, 3H); IR data ν (cm^{-1}) 3379 (−OH),1581, 1512, 1414 (Ar),1270, 1020 (Ar−C−O−C); HRMS (ESI) m/z [M − H]$^-$ calcd. for $[C_{21}H_{19}O_5]^-$ 351.1311, found 351.1225.

*(1E,4Z,6E)-1,7-Bis(3,4-dimethoxypheny1)-5-hydroxyhepta-1,4,6-trien-3-one (**1f**).* Following the general procedure for

https://doi.org/10.1021/acsomega.4c10629
ACS Omega 2024, 9, 51701−51718

the synthesis of Cur derivatives, the corresponding benzaldehyde is veratraldehyde (6.64 g, 40 mmol), and compound **1f** (28.8%) was afforded after purification by column chromatography (petroleum ether/EtOAc, 2:1) as a yellow solid; mp 164−168 °C. ^{1}H NMR (600 MHz, $CDCl_3$) δ 7.61 (d, J = 15.7 Hz, 2H), 7.15 (d, J = 8.4 Hz, 2H), 7.08 (s, 2H), 6.89 (d, J = 8.3 Hz, 2H), 6.50 (d, J = 15.7 Hz, 2H), 5.83 (s, 1H), 3.94 (s, 6H), 3.93 (s, 6H); IR data ν (cm^{-1}) 2940, 2870 (−CH_3), 1621 (—C═O), 1557, 1498 (Ar), 1270, 1022 (Ar−C−O−C); HRMS (ESI) m/z $[M - H]^+$ calcd. for $[C_{23}H_{25}O_2]^+$ 397.1573, found 397.1652.

*(1E,4Z,6E)-1,7-Bis(3,4-dimethylphenyl)-5-hydroxyhepta-1,4,6-trien-3-one (**1g**).* Following the general procedure for the synthesis of Cur derivatives, the corresponding benzaldehyde is 3,4-dimethyl-benzaldehyde (5.37 g, 40 mmol), and compound **1g** (24.8%) was afforded after purification by recrystallization (EtOH/H_2O) as a yellow solid; mp 164−168 °C. ^{1}H NMR (400 MHz, $CDCl_3$) δ 7.64 (d, J = 15.8 Hz, 2H), 7.36 (s, 2H), 7.33 (d, J = 7.7 Hz, 2H), 7.18 (d, J = 7.7 Hz, 2H), 6.61 (d, J = 15.8 Hz, 2H), 5.84 (s, 1H), 2.32 (s, 12H); IR data ν (cm^{-1}) 2940, 2870 (−CH_3), 1621 (—C═O), 1557, 1498 (Ar); HRMS (ESI) m/z $[M - H]^+$ calcd. for $[C_{23}H_{24}O_2]^+$ 333.1776, found 333.1855.

*(1E,4Z,6E)-5-Hydroxy-1,7-bis(4-isopropylphenyl)hepta-1,4,6-trien-3-one (**1h**).* Following the general procedure for the synthesis of Cur derivatives, the corresponding benzaldehyde is *p*-isopropylbenzaldehyde (5.93 g, 40 mmol), and compound **1h** (8.0%) was afforded after purification by column chromatography (petroleum ether/EtOAc, 5:1) as a yellow solid; mp 137−139 °C. ^{1}H NMR (400 MHz, $CDCl_3$) δ 7.68 (d, J = 15.9 Hz, 2H), 7.53 (d, J = 1.9 Hz, 2H), 7.51 (d, J = 2.0 Hz, 2H), 7.29 (d, J = 1.8 Hz, 2H), 7.28 (d, J = 1.9 Hz, 2H), 6.62 (d, J = 15.8 Hz, 2H), 5.86 (s, 1H), 2.96 (hept, J = 7.0 Hz, 2H), 1.30 (s, 6H), 1.28 (s, 6H); IR data ν (cm^{-1}) 2953, 2867 (C−CH_3), 2923, 2867 (C−CH_2−C), 1628 (—C═O), 1580, 1512, 1420 (Ar); HRMS (ESI) m/z $[M - H]^-$ calcd. for $[C_{25}H_{29}O_2]^-$ 361.2089, found 361.2168.

*(1E,4Z,6E)-1,7-Bis(4-(tert-butyl)phenyl)-5-hydroxyhepta-1,4,6-trien-3-one (**1i**).* Following the general procedure for the synthesis of Cur derivatives, the corresponding benzaldehyde is *p-tert*-butylbenzaldehyde (6.49 g, 40 mmol), and compound **1i** (3.6%) was afforded after purification by petroleum ether as a yellow solid; mp 179−182 °C. ^{1}H NMR (400 MHz, $CDCl_3$) δ 7.68 (d, J = 15.9 Hz, 2H), 7.53 (d, J = 8.4 Hz, 4H), 7.45 (d, J = 8.4 Hz, 4H), 6.63 (d, J = 15.9 Hz, 2H), 5.87 (s, 1H), 1.36 (s, 18H); IR data ν (cm^{-1}) 2960, 2870 (−CH_3), 1627 (—C═O), 1398, 1363 (Ar−C(CH_3)$_3$); HRMS (ESI) m/z $[M - H]^+$ calcd. for $[C_{27}H_{33}O_2]^+$ 389.2402, found 389.2481.

*(1E,4Z,6E)-5-Hydroxy-1,7-diphenylhepta-1,4,6-trien-3-one (**1j**).* Following the general procedure for the synthesis of Cur derivatives, the corresponding benzaldehyde is benzaldehyde (5.62 g, 40 mmol), and compound **1j** (33.5%) was afforded after purification by petroleum ether as a yellow solid; mp 130−134 °C. ^{1}H NMR (400 MHz, $CDCl_3$) δ 7.68 (d, J = 15.9 Hz, 2H), 7.57 (d, J = 7.9 Hz, 4H), 7.40 (d, J = 6.4 Hz, 4H), 6.64 (d, J = 15.9, 1.5 Hz, 2H), 5.86 (d, J = 1.5 Hz, 1H); IR data ν (cm^{-1}) 1627 (—C═O), 1580, 1500, 1420 (Ar). The ^{1}H NMR data of compound **1j** are consistent with the reported literature values.[47]

*(1E,4Z,6E)-1,7-Bis(4-bromophenyl)-5-hydroxyhepta-1,4,6-trien-3-one (**1k**).* Following the general procedure for the synthesis of Cur derivatives, the corresponding benzaldehyde is *p*-bromobenzaldehyde (7.40 g, 40 mmol), and compound **1k** (5.1%) was afforded after purification by recrystallization (EtOH/H_2O) as a yellow solid; mp 225−230 °C. ^{1}H NMR (400 MHz, $CDCl_3$) δ 7.60 (d, J = 15.9 Hz, 2H), 7.53 (d, J = 8.5 Hz, 4H), 7.42 (d, J = 8.5 Hz, 4H), 6.61 (d, J = 15.8 Hz, 2H), 5.83 (s, 1H); IR data ν (cm^{-1}) 1628 (—C═O), 1580, 1483, 1400 (Ar), 726 (−Br). The ^{1}H NMR data of compound **1k** are consistent with the reported literature values.[48]

*(1E,4Z,6E)-1,7-Bis(4-chlorophenyl)-5-hydroxyhepta-1,4,6-trien-3-one (**1l**).* Following the general procedure for the synthesis of Cur derivatives, the corresponding benzaldehyde is *p*-chlorobenzaldehyde (4.25 g, 40 mmol), and compound **1l** (5.1%) was afforded after purification by recrystallization (EtOH/H_2O) as a yellow solid; mp 213-216 °C. ^{1}H NMR (400 MHz, DMSO-d_6) δ 7.80 (d, J = 8.5 Hz, 4H), 7.67 (d, J = 16.0 Hz, 2H), 7.54 (d, J = 8.5 Hz, 4H), 7.02 (d, J = 16.0 Hz, 2H), 6.21 (s, 1H); IR data ν (cm^{-1}) 1635 (—C═O), 1580, 1480, 1400 (Ar), 717 (−Cl). The ^{1}H NMR data of compound **1l** are consistent with the reported literature values.[48]

*(1E,4Z,6E)-1,7-Bis(4-fluorophenyl)-5-hydroxyhepta-1,4,6-trien-3-one (**1m**).* Following the general procedure for the synthesis of Cur derivatives, the corresponding benzaldehyde is *p*-fluorobenzaldehyde (4.96 g, 40 mmol), and compound **1m** (13.8%) was afforded after purification by recrystallization (EtOH/H_2O) as a yellow solid; mp 163−167 °C. ^{1}H NMR (400 MHz, $CDCl_3$) δ 7.61 (d, J = 15.8 Hz, 2H), 7.53 (dd, J = 8.6, 5.5 Hz, 4H), 7.07 (t, J = 8.6 Hz, 4H), 6.53 (d, J = 15.8 Hz, 2H), 5.80 (s, 1H); IR data ν (cm^{-1}) 1627 (—C═O), 1582, 1508, 1420 (Ar), 1220 (Ar−C−O), 1151 (−F). The ^{1}H NMR data of compound **1m** are consistent with the reported literature values.[49]

*4.1.2. General Procedure for the Synthesis of **2a**−**2e**.* To a solution of EDCI (0.69 g, 3.6 mmol) was added anhydrous DCM (120 mL). Et_3N (1 mL), Fc-COOH (ferrocenecarboxylic acid, 0.83 g, 3.6 mmol), and DMAP (0.44 g, 3.6 mmol) were added under water bath (0−5 °C) and stirred for 0.5 h. Then the Cur analogue (**1a**−**1e**, 3 mmol) was added, and the mixture was stirred for about 16 h. The whole reaction process was monitored for completion by TLC. At the end, the reaction mixture was quenched with a hydrochloric acid solution (10 mL, 1 N) and then extracted with EtOAc several times. Saturated $NaHCO_3$ solution was used to remove Fc-COOH. The organic phase was washed with saturated NaCl solution several times. Then the combined organic phase was combined, dried over anhydrous $MgSO_4$, and concentrated *in vacuo*.

*Cyclopenta-2,4-dien-1-yl(2-((4-((1E,6E)-7-(4-hydroxy-3-methoxyphenyl)-3,5-dioxohepta-1,6-dien-1-yl)-2-methoxyphenoxy)carbonyl)cyclopenta-2,4-dien-1-yl)iron (**2a**).* Following the general procedure for the synthesis of **2a**−**2e**, the Cur analogue was **1a**, and compound **2a** (23.2%) was afforded after purification by column chromatography (petroleum ether/EtOAc, 2:1) as a yellow solid; mp 187−188 °C. ^{1}H NMR (400 MHz, $CDCl_3$) δ 7.61 (dd, J = 15.8, 8.6 Hz, 2H), 7.18 (d, J = 8.6 Hz, 1H), 7.14 (d, J = 12.9 Hz, 1H), 7.10 (s, 1H), 7.06 (d, J = 15.3 Hz, 2H), 6.92 (d, J = 8.2 Hz, 1H), 6.56 (d, J = 15.8 Hz, 1H), 6.48 (d, J = 15.8 Hz, 1H), 5.83 (s, 1H), 4.94 (t, J = 2.0 Hz, 2H), 4.48 (t, J = 2.0 Hz, 2H), 4.33 (s, 5H), 3.93 (d, J = 7.1 Hz, 6H); IR data ν (cm^{-1}) 3432 (−OH), 2850 (−OCH_3), 1724 (—C═O, Cur), 1627 (—C═O), 1588, 1512, 1449 (Ar), 1273, 1021 (Ar−C−O−C), 486 (ferrocene); HRMS (ESI) m/z $[M - H]^+$ calcd. for $[C_{33}H_{31}FeO_7]^+$ 581.1184, found 581.1263.

https://doi.org/10.1021/acsomega.4c10629
ACS Omega 2024, 9, 51701−51718

*Cyclopenta-2,4-dien-1-yl(2-((4-((1E,6E)-7-(3,4-dimethoxyphenyl)-3,5-dioxohepta-1,6-dien-1-yl)-2-methoxyphenoxy)carbonyl)cyclopenta-2,4-dien-1-yl)iron (**2b**).* Following the general procedure for the synthesis of **2a**−**2e**, the Cur analogue was **1b**, and compound **2b** (10.8%) was afforded after purification by column chromatography (petroleum ether/EtOAc, 2:1) as an orange solid; mp 196−198 °C. ^{1}H NMR (400 MHz, $CDCl_3$) δ 7.69 (d, J = 3.7 Hz, 1H), 7.65 (d, J = 3.6 Hz, 1H), 7.23 (d, J = 14.1 Hz, 2H), 7.17 (d, J = 10.2 Hz, 1H), 7.13 (d, J = 4.5 Hz, 1H), 6.92 (d, J = 8.3 Hz, 1H), 6.62 (d, J = 15.6 Hz, 1H), 6.55 (d, J = 15.9 Hz, 1H), 5.89 (s, 1H), 4.99 (t, J = 2.0 Hz, 2H), 4.58−4.49 (m, 2H), 4.39 (s, 5H), 3.98 (s, 3H), 3.97 (s, 3H), 3.96 (s, 3H); ^{13}C NMR (126 MHz, Chloroform-d) δ 184.29, 182.09, 169.57, 151.88, 151.17, 149.28, 141.35, 140.90, 139.64, 133.92, 127.99, 124.19, 123.74, 122.79, 122.10, 121.06, 111.50, 111.16, 109.80, 101.59, 71.95, 70.74, 70.18, 69.74, 56.02, 55.95, 55.81, 29.71; IR data ν (cm^{-1}) 3451 (−OH), 2823 (−OCH_3), 1727 (—C═O, Cur), 1628 (—C═O), 1580, 1515, 1457 (Ar), 1270, 1023 (Ar−C−O−C), 483 (ferrocene). HRMS (ESI) m/z $[M - H]^+$ calcd. for $[C_{33}H_{31}FeO_7]^+$ 594.1314, found 594.1360.

*Cyclopenta-2,4-dien-1-yl(2-((4-((1E,6E)-7-(4-hydroxyphenyl)-3,5-dioxohepta-1,6-dien-1-yl)phenoxy)carbonyl)cyclopenta-2,4-dien-1-yl)iron (**2c**).* Following the general procedure for the synthesis of **2a**−**2e**, the Cur analogue was **1c**, and compound **2c** (13.9%) was afforded after purification by column chromatography (petroleum ether/EtOAc, 2:1) as a yellow solid; mp 215−226 °C. ^{1}H NMR (400 MHz, DMSO-d_6) δ 7.83 (d, J = 8.4 Hz, 2H), 7.69−7.63 (m, 1H), 7.60 (d, J = 8.4 Hz, 2H), 7.32 (d, J = 8.4 Hz, 2H), 6.95 (d, J = 15.8 Hz, 1H), 6.84 (d, J = 8.4 Hz, 2H), 6.75 (d, J = 15.8 Hz, 1H), 6.15 (s, 1H), 4.95 (t, J = 1.9 Hz, 2H), 4.65 (t, J = 1.9 Hz, 2H), 4.38 (s, 5H); ^{13}C NMR (126 MHz, DMSO-d_6) δ 185.32, 181.94, 169.98, 160.47, 152.47, 152.33, 141.66, 139.17, 132.88, 130.97, 129.98, 126.19, 124.83, 124.77, 123.09, 121.32, 116.41, 101.95, 79.71, 79.45, 79.19, 72.73, 70.80, 70.38, 69.67; IR data ν (cm^{-1}) 3420 (−OH), 1728 (—C═O, Cur), 1628 (—C═O), 1580, 1510, 1420 (Ar), 1275, 1020 (Ar−C−O−C), 1218 (Ar−C−O), 493 (ferrocene); HRMS (ESI) m/z $[M - H]^+$ calcd. for $[C_{30}H_{25}FeO_5]^+$ 520.0973, found 520.0995.

*Cyclopenta-2,4-dien-1-yl(2-((4-((1E,6E)-7-(4-hydroxy-3-methoxyphenyl)-3,5-dioxohepta-1,6-dien-1-yl)phenoxy)carbonyl)cyclopenta-2,4-dien-1-yl)iron (**2d**).* Following the general procedure for the synthesis of **2a**−**2e**, the Cur analogue was **1d**, and compound **2d** (20.6%) was afforded after purification by column chromatography (petroleum ether/EtOAc, 2:1) as a yellow solid; mp 146−151 °C. ^{1}H NMR (400 MHz, $CDCl_3$) δ 7.83 (d, J = 8.4 Hz, 1H), 7.69−7.62 (m, 1H), 7.58 (d, J = 8.2 Hz, 1H), 7.34 (q, J = 7.9 Hz, 3H), 7.20 (dd, J = 18.1, 8.2 Hz, 1H), 6.97 (dd, J = 22.4, 16.2 Hz, 1H), 6.86−6.77 (m, 2H), 6.16 (s, 1H), 4.93 (dt, J = 13.8, 2.0 Hz, 2H), 4.63 (dt, J = 10.7, 2.0 Hz, 2H), 4.38 (s, 5H), 3.84 (s, 3H); ^{13}C NMR (126 MHz, $CDCl_3$) δ 184.62, 181.88, 170.23, 158.02, 151.79, 148.02, 146.83, 141.18, 140.84, 139.48, 139.14, 134.06, 132.69, 130.09, 129.23, 127.60, 127.51, 124.18, 123.65, 123.09, 122.30, 121.80, 121.10, 116.01, 114.87, 111.45, 109.70, 70.76, 70.22, 70.05, 69.54, 56.00, 55.79, 29.71; IR data ν (cm^{-1}) 3430 (−OH), 2850 (−OCH_3), 1727 (—C═O, Cur), 1627 (—C═O), 1580, 1512, 1419 (Ar), 1270, 1024 (Ar−C−O−C), 1221 (Ar−C−O), 487 (ferrocene). HRMS (ESI) m/z $[M - H]^+$ calcd. for $[C_{31}H_{27}FeO_6]^+$ 550.1079, found 550.1114.

*Cyclopenta-2,4-dien-1-yl(2-((4-((1E,6E)-7-(3,4-dimethoxyphenyl)-3,5-dioxohepta-1,6-dien-1-yl)phenoxy)carbonyl)cyclopenta-2,4-dien-1-yl)iron (**2e**).* Following the general procedure for the synthesis of **2a**−**2e**, the Cur analogue was **1e**, and compound **2e** (11.3%) was afforded after purification by column chromatography (petroleum ether/EtOAc, 2:1) as a yellow solid; mp 100−110 °C. ^{1}H NMR (400 MHz, $CDCl_3$) δ 7.62 (d, J = 14.4 Hz, 2H), 7.58−7.55 (m, 2H), 7.11 (d, J = 8.9 Hz, 1H), 7.05 (s, 1H), 6.84 (d, J = 8.3 Hz, 1H), 6.55 (d, J = 15.9 Hz, 2H), 6.48 (d, J = 15.8 Hz, 2H), 5.80 (s, 1H), 4.92 (t, J = 2.0 Hz, 2H), 4.48 (t, J = 2.0 Hz, 2H), 4.26 (s, 5H), 3.90 (s, 3H), 3.88 (s, 3H); ^{13}C NMR (126 MHz, $CDCl_3$) δ 184.25, 182.19, 170.12, 152.33, 152.24, 151.16, 149.28, 140.88, 139.70, 139.25, 132.59, 132.49, 129.30, 129.22, 128.01, 124.08, 122.82, 122.30, 122.09, 111.16, 109.78, 101.95, 101.66, 72.13, 70.70, 70.02, 69.73, 56.02, 55.96, 29.71, 29.38, 22.71, 14.14; IR data ν (cm^{-1}) 2924, 2850 (−CH_2), 1728 (—C═O, Cur), 1627 (—C═O), 1580, 1512, 1416 (Ar), 1270, 1020 (Ar−C−O−C), 1220 (Ar−C−O), 493 (ferrocene). HRMS (ESI) m/z $[M - H]^+$ calcd. for $[C_{32}H_{29}FeO_6]^+$ 565.1235, found 565.1306.

*4.1.3. General Procedure for the Synthesis of **3a**−**3m**.* To a solution of Cur analogues (**1a**−**1m**, 6 mmol) and ferrocenecarboxaldehyde (Fc-CHO, 0.56 g, 6 mmol) in anhydrous DMF (25 mL) was added piperidine (2 mL) dropwise, and the mixture was stirred for about 48 h. The whole reaction process was monitored for completion by TLC. At the end, the reaction mixture was quenched with glacial acetic acid (5 mL) and then extracted with EtOAc three times, and the organic phase was washed with saturated NaCl solution several times. Then combined organic phase, dried over anhydrous $MgSO_4$, and concentrated *in vacuo*.

*Cyclopenta-2,4-dien-1-yl(2-((E)-5(4-hydroxy-3-methoxyphenyl)-2-((E)-3-(4-hydroxy-3-methoxyphenyl)acryloyl)-3-oxopenta-1,4-dien-1-yl)cyclopenta-2,4-dien-1-yl)iron (**3a**).* Following the general procedure for the synthesis of **3a**−**3m**, the Cur analogue was **1a**, and compound **3a** (7.1%) was afforded after purification by column chromatography (petroleum ether/EtOAc, 2:1) as a purple solid; mp 92−95 °C. ^{1}H NMR (400 MHz, $CDCl_3$) δ 7.77 (d, J = 15.6 Hz, 2H), 7.48 (d, J = 16.2 Hz, 2H), 7.21−7.16 (m, 1H), 7.14−7.08 (m, 1H), 7.05 (s, 2H), 6.85 (d, J = 15.9 Hz, 2H), 4.49 (s, 4H), 4.22 (s, 5H), 3.94 (s, 3H), 3.92 (s, 3H); IR data ν (cm^{-1}) 3422 (−OH), 2850 (−OCH_3), 1627 (—C═O), 1580, 1512, 1423 (Ar), 1272, 1023 (Ar−C−O−C), 1221 (Ar−C−O), 493 (ferrocene); HRMS (ESI) m/z $[M - H]^+$ calcd. for $[C_{32}H_{29}FeO_6]^+$ 564.1235, found 564.1314. The ^{1}H NMR data of compound **3a** are consistent with the reported literature values.[36]

*Cyclopenta-2,4-dien-1-yl(2-((1E,4E)-5(3,4-dimethoxyphenyl)-2-((E)-3-(4-hydroxy-3-methoxyphenyl)acryloyl)-3-oxopenta-1,4-dien-1-yl)cyclopenta-2,4-dien-1-yl)iron (**3b**).* Following the general procedure for the synthesis of **3a**−**3m**, the Cur analogue was **1b**, and compound **3b** (4.1%) was afforded after purification by column chromatography (petroleum ether/EtOAc, 2:1) as a purple solid; mp 92−100 °C. ^{1}H NMR (400 MHz, $CDCl_3$) δ 7.79 (d, J = 15.7 Hz, 2H), 7.49 (s, 1H), 7.13 (s, 1H), 7.07 (d, J = 10.2 Hz, 2H), 6.89 (dd, J = 14.2, 7.9 Hz, 4H), 4.50 (d, J = 6.5 Hz, 4H), 4.23 (s, 5H), 3.96 (s, 3H), 3.94 (s, 3H), 3.93 (s, 3H), 3.51 (s, 1H); ^{13}C NMR (126 MHz, $CDCl_3$) δ 198.80, 185.57, 151.86, 151.43, 149.31, 149.18, 147.29, 147.12, 144.51, 144.34, 142.75, 136.33, 127.95, 127.11, 126.71, 126.03, 125.77, 123.96, 123.60, 123.43, 123.16, 120.56, 120.25, 114.92, 114.82, 111.10, 110.59, 110.04, 72.27, 71.48, 70.01, 56.02, 29.54; IR data ν (cm^{-1}) 3400 (−OH), 2825 (−OCH_3), 1635 (—C═O), 1588, 1512, 1457

https://doi.org/10.1021/acsomega.4c10629
ACS Omega 2024, 9, 51701−51718

(Ar), 1270, 1021 (Ar−C−O−C), 493 (ferrocene). HRMS (ESI) m/z $[M - H]^+$ calcd. for $[C_{33}H_{31}FeO_6]^+$ 578.1392, found 578.1417.

Cyclopenta-2,4-dien-1-yl(2-((E)-5(4-hydroxyphenyl)-2-((E)-3-(4-hydroxyphenyl) acryloyl)-3-oxopenta-1,4-dien-1-yl)cyclopenta-2,4-dien-1-yl)iron (**3c**). Following the general procedure for the synthesis of **3a−3m**, the Cur analogue was **1c**, and compound **3c** was afforded after purification by column chromatography (petroleum ether/EtOAc, 1.5:1) as a purple solid; mp 155−160 °C. ^{1}H NMR (600 MHz, DMSO-d_6) δ 7.87 (s, 1H), 7.67 (s, 2H), 7.63 (s, 2H), 7.53 (d, J = 15.0 Hz, 1H), 7.43 (s, 2H), 6.85 (d, J = 15.0 Hz, 2H), 6.80 (s, 2H), 4.53 (s, 1H), 4.46 (s, 1H), 4.36 (s, 1H), 4.19 (s, 5H), 4.03 (s, 1H); ^{13}C NMR (126 MHz, DMSO-d_6) δ 198.65, 186.83, 160.84, 160.41, 146.84, 143.23, 142.03, 137.84, 132.57, 132.00, 131.38, 131.21, 129.14, 126.32, 125.56, 125.00, 118.74, 116.45, 116.30, 76.89, 72.28, 71.63, 70.11, 65.49, 30.47, 19.12; IR data ν (cm^{-1}) 3415 (−OH), 1628 (—C═O), 1582, 1510, 1420 (Ar), 1220 (Ar−C−O), 495 (ferrocene): HRMS (ESI) m/z $[M - H]^+$ calcd. for $[C_{32}H_{29}FeO_5]^+$ 505.1024, found 505.1102.

Cyclopenta-2,4-dien-1-yl(2-((1E,4E)-5(4-hydroxy-3-methoxyphenyl)-2-((E)-3-(4-hydroxyphenyl)acryloyl)-3-oxopenta-1,4-dien-1-yl)cyclopenta-2,4-dien-1-yl)iron (**3d**). Following the general procedure for the synthesis of **3a−3m**, the Cur analogue was **1d**, and compound **3d** (11.5%) was afforded after purification by column chromatography (petroleum ether/EtOAc, 1.5:1) as a purple solid; mp 130−131 °C. ^{1}H NMR (600 MHz, DMSO-d_6) δ 7.87 (d, J = 13.8 Hz, 1H), 7.67 (d, J = 8.0 Hz, 1H), 7.63 (d, J = 8.0 Hz, 1H), 7.54 (d, J = 15.0 Hz, 1H), 7.46−7.40 (m, 2H), 6.85 (d, J = 10.8 Hz, 2H), 6.81 (d, J = 7.7 Hz, 2H), 4.53 (s, 1H), 4.47 (s, 1H), 4.36 (s, 1H), 4.19 (s, 5H), 4.03 (s, 1H), 3.83 (d, J = 29.2 Hz, 3H); ^{13}C NMR (126 MHz, DMSO-d_6) δ 198.69, 186.79, 160.84, 160.40, 150.35, 149.95, 148.49, 147.26, 146.84, 143.70, 143.22, 142.03, 141.96, 137.91, 137.84, 131.38, 131.20, 126.79, 126.32, 126.09, 125.56, 125.26, 125.00, 124.20, 123.47, 118.99, 118.73, 116.45, 116.30, 116.23, 116.15, 113.12, 112.14, 76.90, 72.27, 71.64, 70.11; IR data ν (cm^{-1}) 3430 (−OH), 2850 (−OCH_3), 1627 (—C═O), 1583, 1512, 1440 (Ar), 1270, 1027 (Ar−C−O−C), 1215 (Ar−C−O), 493 (ferrocene); HRMS (ESI) m/z $[M - H]^+$ calcd. for $[C_{31}H_{27}FeO_5]^+$ 535.1130, found 535.1208.

Cyclopenta-2,4-dien-1-yl(2-((1E,4E)-5(3,4-dimethoxyphenyl)-2-((E)-3-(4-hydroxyphenyl)acryloyl)-3-oxopenta-1,4-dien-1-yl)cyclopenta-2,4-dien-1-yl)iron (**3e**). Following the general procedure for the synthesis of **3a−3m**, the Cur analogue was **1e**, and compound **3e** (12.3%) was afforded after purification by column chromatography (petroleum ether/EtOAc, 1:1) as a purple solid; mp 93−115 °C. ^{1}H NMR (400 MHz, $CDCl_3$) δ 7.82−7.76 (m, 2H), 7.48 (d, J = 8.2 Hz, 2H), 7.42 (d, J = 7.9 Hz, 1H), 7.08 (s, 1H), 6.90 (s, 1H), 6.84 (d, J = 6.9 Hz, 2H), 4.50 (d, J = 1.9 Hz, 4H), 4.23 (s, 5H), 3.94 (s, 3H), 3.92 (s, 3H); ^{13}C NMR (126 MHz, DMSO-d_6) δ 198.65, 186.94, 160.84, 160.41, 149.50, 146.84, 143.29, 143.23, 142.31, 142.10, 142.03, 137.85, 131.38, 131.21, 126.32, 126.13, 125.57, 125.00, 118.74, 116.45, 116.30, 112.20, 112.08, 76.89, 76.79, 72.32, 72.28, 71.69, 71.64, 70.12, 56.30, 56.10, 56.05; IR data ν (cm^{-1}) 3152 (−OH), 2924, 2850 (−CH_2), 1627 (—C═O), 1580, 1512, 1440 (Ar), 1270, 1020 (Ar−C−O−C), 1218 (Ar−C−O), 493 (ferrocene). HRMS (ESI) m/z $[M - H]^+$ calcd. for $[C_{32}H_{29}FeO_5]^+$ 548.1286, found 548.1312.

Cyclopenta-2,4-dien-1-yl(2-((E)-5(3,4-dimethoxyphenyl)-2-((E)-3-(3,4-dimethoxyphenyl)acryloyl)-3-oxopenta-1,4-dien-1-yl)cyclopenta-2,4-dien-1-yl)iron (**3f**). Following the general procedure for the synthesis of **3a−3m**, the Cur analogue was **1f**, and compound **3f** (18.4%) was afforded after purification by column chromatography (petroleum ether/EtOAc, 1:1) as a brown solid; mp 94−100 °C. ^{1}H NMR (400 MHz, $CDCl_3$) δ 7.78 (d, J = 16.3 Hz, 2H), 7.50 (d, J = 16.1 Hz, 1H), 7.21 (dd, J = 8.4, 2.0 Hz, 1H), 7.13 (dd, J = 8.4, 2.0 Hz, 1H), 7.08 (d, J = 2.0 Hz, 2H), 6.91 (d, J = 8.7 Hz, 1H), 6.89 (d, J = 4.7 Hz, 1H), 6.86 (d, J = 5.3 Hz, 1H), 4.53- 4.50 (m, 2H), 4.50−4.47 (m, 2H), 4.23 (s, 5H), 3.93 (s, 6H), 3.92 (d, J = 2.1 Hz, 6H); IR data ν (cm^{-1}) 2825 (−OCH_3), 1628 (—C═O), 1585, 1512, 1426 (Ar), 1264, 1020 (Ar−C−O−C),493 (ferrocene). HRMS (ESI) m/z $[M - H]^+$ calcd. for $[C_{34}H_{33}FeO_6]^+$ 592.1548, found 592.1561. The ^{1}H NMR data of compound **3f** are consistent with the reported literature values.[36]

Cyclopenta-2,4-dien-1-yl(2-((E)-5(3,4-dimethylphenyl)-2-((E)-3-(3,4-dimethylphenyl)acryloyl)-3-oxopenta-1,4-dien-1-yl)cyclopenta-2,4-dien-1-yl)iron (**3g**). Following the general procedure for the synthesis of **3a−3m**, the Cur analogue was **1g**, and compound **3g** (11.3%) was afforded after purification by column chromatography (petroleum ether/EtOAc, 5/1) as an amaranth solid; mp 69−75 °C. ^{1}H NMR (400 MHz, $CDCl_3$) δ 7.78 (d, J = 17.1 Hz, 2H), 7.51 (d, J = 16.2 Hz, 1H), 7.35 (d, J = 5.8 Hz, 2H), 7.32 (s, 1H), 7.15 (d, J = 7.7 Hz, 2H), 6.99 (d, J = 12.3 Hz, 1H), 6.95 (d, J = 13.1 Hz, 1H), 4.52−4.48 (m, 2H), 4.47 (t, J = 1.9 Hz, 2H), 4.22 (s, 5H), 2.29 (s, 6H), 2.28 (d, J = 4.9 Hz, 6H); ^{13}C NMR (126 MHz, $CDCl_3$) δ 198.95, 185.73, 147.26, 144.42, 142.87, 140.49, 139.82, 137.34, 137.14, 136.36, 132.59, 131.88, 130.32, 130.16, 129.91, 129.71, 126.94, 126.37, 126.35, 121.44, 76.41, 72.27, 71.49, 70.00, 26.93; IR data ν (cm^{-1}) 2945, 2870 (−CH_3), 1621 (—C═O), 1512, 1457 (Ar), 1263, 1022 (Ar−C−O−C), 493 (ferrocene). HRMS (ESI) m/z $[M - H]^+$ calcd. for $[C_{34}H_{33}FeO_2]^+$ 528.1752, found 528.1771.

Cyclopenta-2,4-dien-1-yl(2-((E)-5(4-isopropylphenyl)-2-((E)-3-(4-isopropylphenyl)acryloyl)-3-oxopenta-1,4-dien-1-yl)cyclopenta-2,4-dien-1-yl)iron (**3h**). Following the general procedure for the synthesis of **3a−3m**, the Cur analogue was **1h**, and compound **3h** was afforded after purification by column chromatography (petroleum ether/EtOAc, 3:1) as an amaranth solid; mp 58−68 °C. ^{1}H NMR (400 MHz, $CDCl_3$) δ 7.85−7.76 (m, 1H), 7.54 (d, J = 12.2 Hz, 1H), 7.51 (d, J = 4.2 Hz, 1H), 7.49 (d, J = 8.1 Hz, 1H), 7.25 (d, J = 8.1 Hz, 2H), 7.22−7.15 (m, 1H), 7.05 (d, J = 26.5 Hz, 1H), 6.96 (d, J = 15.9 Hz, 1H), 4.82 (t, J = 1.9 Hz, 1H), 4.63 (t, J = 1.9 Hz, 1H), 4.48 (h, J = 1.9 Hz, 2H), 4.27 (d, J = 30.8 Hz, 5H), 2.99−2.87 (m, 2H), 1.26 (t, J = 6.6 Hz, 12H); ^{13}C NMR (126 MHz, $CDCl_3$) δ 198.75, 193.32, 185.49, 152.44, 151.76, 146.83, 144.03, 142.90, 136.06, 132.44, 131.71, 128.64, 127.00, 126.86, 121.58, 73.06, 72.18, 71.33, 69.87, 69.53, 68.92, 34.01, 29.57, 23.60; IR data ν (cm^{-1}) 2960, 2863 (C−CH_3), 2924, 2863 (C−CH_2−C), 1650 (—C═O), 1590, 1512, 1440 (Ar), 1280, 1030 (Ar−C−O−C), 491 (ferrocene). HRMS (ESI) m/z $[M - H]^+$ calcd. for $[C_{36}H_{37}FeO_2]^+$ 557.2065, found 557.2121.

Cyclopenta-2,4-dien-1-yl(2-((E)-5(4-(tert-butyl)phenyl)-2-((E)-3-(4-(tert-butyl)phenyl)acryloyl)-3-oxopenta-1,4-dien-1-yl)cyclopenta-2,4-dien-1-yl)iron (**3i**). Following the general procedure for the synthesis of **3a−3m**, the Cur analogue was **1i**, and compound **3i** was afforded after purification by column chromatography (petroleum ether/EtOAc, 3:1) as an amaranth solid; mp 90−95 °C. ^{1}H NMR (400 MHz, $CDCl_3$) δ 7.74−7.68 (m, 2H), 7.46 (d, J = 10.5 Hz, 2H), 7.42 (d, J = 2.6

https://doi.org/10.1021/acsomega.4c10629
ACS Omega 2024, 9, 51701−51718

Hz, 2H), 7.40 (d, J = 8.5 Hz, 2H), 7.32 (d, J = 8.2 Hz, 4H), 6.91 (d, J = 12.6 Hz, 1H), 6.87 (d, J = 13.2 Hz, 1H), 4.39 (dq, J = 3.6, 1.9 Hz, 4H), 4.13 (s, 5H), 1.24 (d, J = 6.1 Hz, 18H); ^{13}C NMR (126 MHz, $CDCl_3$) δ 198.79, 185.50, 154.70, 154.00, 146.75, 143.92, 142.95, 136.04, 132.05, 131.32, 128.45, 127.06, 125.91, 121.74, 72.19, 71.34, 69.88, 34.83, 30.99, 29.58; IR data ν (cm^{-1}) 2960, 2870 (−CH_3), 1638 (—C═O), 1588, 1515, 1441 (Ar), 1395, 1365 (Ar−C(CH_3)$_3$), 498 (ferrocene). HRMS (ESI) m/z $[M - H]^+$ calcd. for $[C_{38}H_{41}FeO_2]^+$ 584.2378, found 584.2473.

(2-((E)-2-Cinnamoyl-3-oxo-5-phenylpenta-1,4-dien-1-yl)-cyclopenta-2,4-dien-1-yl)(cyclopenta-2,4-dien-1-yl)iron ***(3j)***. Following the general procedure for the synthesis of **3a−3m**, the Cur analogue was **1j**, and compound **3j** was afforded after purification by column chromatography (petroleum ether/EtOAc, 5:1) as a purple solid; mp 80−85 °C. ^{1}H NMR (400 MHz, $CDCl_3$) δ 7.76−7.70 (m, 2H), 7.53−7.43 (m, 6H), 7.32−7.30 (m, 4H), 6.98 (d, J = 15.5 Hz, 1H), 6.89 (d, J = 16.3 Hz, 1H), 4.41 (s, 4H), 4.14 (s, 5H); ^{13}C NMR (126 MHz, $CDCl_3$) δ 198.64, 185.67, 146.69, 144.13, 143.52, 141.39, 136.05, 134.91, 134.39, 134.21, 131.03, 130.64, 130.50, 129.04, 128.90, 128.82, 128.78, 128.73, 128.68, 128.57, 127.87, 122.41, 76.25, 72.49, 71.54, 70.08, 29.71; IR data ν (cm^{-1}) 1627 (—C═O), 1580, 1505, 1420 (Ar), 1220 (Ar−C−O), 480 (ferrocene). HRMS (ESI) m/z $[M - H]^+$ calcd. for $[C_{30}H_{25}FeO_2]^+$ 473.1126, found 473.1224.

(2-((E)-5-(4-Bromophenyl)-2-((E)-3-(4-bromophenyl)-acryloyl)-3-oxopenta-1,4-dien-1-yl)cyclopenta-2,4-dien-1-yl)(cyclopenta-2,4-dien-1-yl)iron ***(3k)***. Following the general procedure for the synthesis of **3a−3m**, the Cur analogue was **1k**, and compound **3k** (2%) was afforded after purification by column chromatography (petroleum ether/EtOAc, 5:1) as a brown solid; mp 75−83 °C. ^{1}H NMR (400 MHz, $CDCl_3$) δ 7.81 (s, 1H), 7.71 (d, J = 15.5 Hz, 2H), 7.52 (d, J = 4.1 Hz, 1H), 7.50 (d, J = 4.2 Hz, 2H), 7.45−7.42 (m, 2H), 7.38 (d, J = 8.5 Hz, 2H), 6.92 (d, J = 16.1 Hz, 2H), 4.53−4.49 (m, 2H), 4.47 (t, J = 1.9 Hz, 2H), 4.21 (s, 5H); ^{13}C NMR (126 MHz, $CDCl_3$) δ 198.12, 185.48, 144.94, 144.16, 142.73, 135.79, 133.79, 133.10, 132.42, 132.31, 132.17, 131.00, 129.96, 129.92, 128.23, 125.43, 124.80, 122.79, 76.18, 72.76, 71.63, 70.19, 29.71; IR data ν (cm^{-1}) 2925, 2856 (−CH_3), 1638 (—C═O), 1588, 1510, 1440 (Ar), 1270, 1025 (Ar−C−O−C), 77 (−Br), 491 (ferrocene). HRMS (ESI) m/z $[M - H]^+$ calcd. for $[C_{30}H_{22}Br_2FeO_2]^+$ 630.9316, found 630.9448.

(2-((E)-5-(4-Chlorophenyl)-2-((E)-3-(4-chlorophenyl)-acryloyl)-3-oxopenta-1,4-dien-1-yl)cyclopenta-2,4-dien-1-yl)(cyclopenta-2,4-dien-1-yl)iron ***(3l)***. Following the general procedure for the synthesis of **3a−3m**, the Cur analogue was **1l**, and compound **3l** (34.4%) was afforded after purification by column chromatography (petroleum ether/EtOAc, 5:1) as a purple solid; mp 70−79 °C. ^{1}H NMR (400 MHz, $CDCl_3$) δ 7.81 (s, 1H), 7.73 (d, J = 15.5 Hz, 2H), 7.50 (s, 2H), 7.47−7.43 (m, 3H), 7.36−7.33 (m, 4H), 6.90 (d, J = 16.3 Hz, 2H), 4.51 (s, 2H), 4.47 (s, 2H), 4.21 (s, 5H); ^{13}C NMR (126 MHz, $CDCl_3$) δ 198.24, 185.57, 145.00, 144.18, 142.77, 136.52, 135.92, 133.47, 132.78, 129.86, 129.38, 128.27, 122.81, 72.81, 71.71, 70.27, 29.81; IR data ν (cm^{-1}) 1630 (—C═O), 1588, 1498, 1420 (Ar), 1270, 1020 (Ar−C−O−C), 669 (Ar−Cl), 488 (ferrocene). HRMS (ESI) m/z $[M - H]^+$ calcd. for $[C_{30}H_{22}Cl_2FeO_2]^+$ 540.0346, found 540.0381.

Cyclopenta-2,4-dien-1-yl(2-((E)-5-(4-fluorophenyl)-2-((E)-3-(4-fluorophenyl)acryloyl)-3-oxopenta-1,4-dien-1-yl)-cyclopenta-2,4-dien-1-yl) iron ***(3m)***. Following the general procedure for the synthesis of **3a−3m**, the Cur analogue was **1m**, and compound **3m** (5%) was afforded after purification by column chromatography (petroleum ether/EtOAc, 5:1) as a purple solid; mp 155−158 °C. ^{1}H NMR (400 MHz, $CDCl_3$) δ 7.83 (s, 1H), 7.78 (d, J = 15.5 Hz, 1H), 7.60 (d, J = 8.5 Hz, 2H), 7.56 (d, J = 7.3 Hz, 1H), 7.53 (s, 1H), 7.51 (d, J = 10.6 Hz, 1H), 7.09 (td, J = 8.6, 3.4 Hz, 4H), 6.99 (d, J = 15.4 Hz, 1H), 6.89 (d, J = 16.2 Hz, 1H), 4.53−4.51 (m, 2H), 4.50 (s, 2H), 4.26−4.21 (m, 5H); ^{13}C NMR (126 MHz, $CDCl_3$) δ 198.33, 185.48, 165.33, 165.05, 163.32, 163.05, 145.21, 143.71, 142.84, 135.93, 131.15, 130.66, 130.60, 130.52, 130.46, 127.59, 122.05, 116.36, 116.18, 116.00, 76.21, 72.59, 71.55, 70.13, 31.94, 31.45, 30.20, 29.71; IR data ν (cm^{-1}) 1627 (—C═O), 1583, 1510, 1418 (Ar), 1221 (Ar−C−O), 1155 (Ar−F), 497 (ferrocene). HRMS (ESI) m/z $[M - H]^+$ calcd. for $[C_{30}H_{22}F_2FeO_2]^+$ 509.0937, found 509.1038.

4.2. Evaluation. Human normal colon epithelial cell line NCM460, human monocytic leukemia THP-1 cell line, human CRC cell lines SW480 and RKO, mouse CRC CT26 cell line, and mouse mononuclear macrophage cell RAW264.7 were all purchased from the Cell Bank of the Chinese Academy of Sciences.

4.2.1. Preparation of Compounds. Appropriate amounts of solid powder of Cur, CVB-D, and ferrocenyl-substituted Cur derivatives (**2a−2e**, and **3a−3m**) were weighed and placed in labeled centrifuge tubes. First, a certain volume of DMSO was used to completely dissolve the compounds, and then an appropriate amount of cell culture medium was added. The concentration was 10 mmol/L, and the 0.22 μM filter was filtered, sterilized, and stored in a plastic bag in a −20 °C refrigerator for use later. When administering cells *in vitro*, thaw at room temperature and dilute the drug mother solution proportionally with cell culture to the desired concentration.

4.2.2. Cell lines and Cell Culture. Human normal colon epithelial cell line NCM460, monocytic leukemia THP-1 cell line, human CRC cell lines SW480 and RKO, mouse mononuclear macrophage cell RAW264.7, and mouse CRC cell line CT26 were taken out from cryopreservation tubes frozen at −80 °C and shaken in a 37 °C constant temperature water bath to thaw and resuscitate the cells quickly.

First, the thawed cell cryovials were centrifuged at 1000 r/min for 5 min and aseptically operated on a clean bench. Then, the original cryopreservation solution was discarded, and the cells were resuspended in the DMEM complete medium containing 10% FBS and 1% penicillin/streptomycin bispecific antibody. Next, cells were seeded into T25 cell culture flasks and cultured in a 37 °C and 5% CO_2 in a cell culture incubator. Observe the growth state of the cells; when the cells grow adherently and the degree of confluence reaches 80−90%, the cell subculture is carried out, and the complete medium is replaced in time according to the growth and survival status of the cells.

4.2.3. MTT Assay. NCM460, HTP-1, SW480, RKO, RAW264.7 and CT26 cells were trypsinized, the cell density was adjusted to 5×10^3 to 6×10^3 cells/mL. 100 μL/well cell suspension was randomly and uniformly seeded in 96-well cell culture plates. Cells were cultured in media containing different drug concentrations, and an equal volume of solvent was added as control group. After treatment and incubation, the cell morphology was observed, and the number of cells in each well was measured. Next, MTT reagent was added, and the mixture was further incubated to metabolize into a purple precipitate. After the sample was washed, DMSO was added to

https://doi.org/10.1021/acsomega.4c10629
ACS Omega 2024, 9, 51701−51718

the mix, and cell viability was assessed by measuring absorbance values.

4.2.4. Western Blot Assay. CRC cells seeded at a density of 3×10^5 to 5×10^5/mL were cultured until completely adherent, and the cells were randomly intervened and continued to be cultured for 24 h. Next, the protein was collected from the cells, and the concentration of protein was measured by the BCA protein quantitation method and adjusted. The proteins were denatured by boiling, separated by SDS-PAGE gel electrophoresis, transferred to PVDF membranes, and finally detected by peroxidase labeling.

4.2.5. Statistical Analysis. Rigorous statistical methods and GraphPad Prism 8 software for one-way ANOVA or *t* test are used to analyze the data. Experimental results are presented as mean ± standard deviations, and at least three independent replicates of the experiment are performed. At the significance level $p < 0.05$, the signs "*" and "#" are used to indicate that the difference is statistically significant. At the significance level $p < 0.01$, the symbols "**" and "##" indicate very significant; at the significance level $p < 0.001$, the use of the symbols "***" and "###" indicates extremely significant.

■ ASSOCIATED CONTENT

Data Availability Statement

The data underlying this study are available in the published article and its Supporting Information.

Supporting Information

The Supporting Information is available free of charge at https://pubs.acs.org/doi/10.1021/acsomega.4c10629.

^{1}H NMR, ^{13}C NMR, HRMS, and FT-IR spectra for all compounds (PDF)

■ AUTHOR INFORMATION

Corresponding Authors

Xue-Jie Qi − *Tianjin Key Laboratory of Therapeutic Substance of Traditional Chinese Medicine, School of Chinese Materia Medica, Tianjin University of Traditional Chinese Medicine, Tianjin 301617, P. R. China; State Key Laboratory of Chinese Medicine Modernization, Tianjin 301617, P. R. China;* orcid.org/0000-0003-2063-4046; Email: qixuejie2014@163.com

Lili Duan − *Tianjin Key Laboratory of Therapeutic Substance of Traditional Chinese Medicine, School of Chinese Materia Medica, Tianjin University of Traditional Chinese Medicine, Tianjin 301617, P. R. China;* orcid.org/0009-0006-8975-9532; Email: lduan2020@tjutcm.edu.cn

Yuye Li − *Binhai New Area Hospital of TCM, Tianjin 300451, China*; Email: liyuye1025@163.com

Authors

Xing-Ze Zhang − *Tianjin Key Laboratory of Therapeutic Substance of Traditional Chinese Medicine, School of Chinese Materia Medica, Tianjin University of Traditional Chinese Medicine, Tianjin 301617, P. R. China*

Gen Li − *Tianjin Key Laboratory of Therapeutic Substance of Traditional Chinese Medicine, School of Chinese Materia Medica, Tianjin University of Traditional Chinese Medicine, Tianjin 301617, P. R. China*

Gao-Yong Hu − *State Key Laboratory of Component-based Chinese Medicine, Research Center of Traditional Chinese Medicine, Tianjin University of Traditional Chinese Medicine, Tianjin 301617, P. R. China*

Chen-Lin Wang − *Tianjin Key Laboratory of Therapeutic Substance of Traditional Chinese Medicine, School of Chinese Materia Medica, Tianjin University of Traditional Chinese Medicine, Tianjin 301617, P. R. China*

Yu-Qiu Fang − *Tianjin Key Laboratory of Therapeutic Substance of Traditional Chinese Medicine, School of Chinese Materia Medica, Tianjin University of Traditional Chinese Medicine, Tianjin 301617, P. R. China*

Complete contact information is available at: https://pubs.acs.org/10.1021/acsomega.4c10629

Author Contributions

#X.-Z.Z., G.L., and G.-Y.H. contributed equally.

Notes

The authors declare no competing financial interest.

■ ACKNOWLEDGMENTS

We are grateful to Tianjin Municipal Health Commission (Grant No. 2023077), the National Natural Science Foundation of China (82074281), and Tianjin Municipal Education Commission (No. 2022ZD041) for financial support. We would like to thank the Core Technology Facility of Tianjin University of Traditional Chinese Medicine.

■ REFERENCES

(1) Singh, N.; Baby, D.; Rajguru, J. P.; Patil, P. B.; Thakkannavar, S. S.; Pujari, V. B. Inflammation and cancer. *Ann. Afr. Med.* **2019**, *18*, 121−126.

(2) Zhao, H.; Wu, L.; Yan, G.; et al. Inflammation and tumor progression: signaling pathways and targeted intervention. *Signal Transduct Target Ther.* **2021**, *6*, 263.

(3) Dallavalasa, S.; Beeraka, N. M.; Basavaraju, C. G.; et al. The Role of Tumor Associated Macrophages (TAMs) in Cancer Progression, Chemoresistance, Angiogenesis and Metastasis - Current Status. *Curr. Med. Chem.* **2021**, *28*, 8203−8236.

(4) Song, J.; Lan, J.; Tang, J.; Luo, N. PTPN2 in the Immunity and Tumor Immunotherapy: A Concise Review. *Int. J. Mol. Sci.* **2022**, *23*, 10025.

(5) Matozaki, T.; Murata, Y.; Saito, Y.; Okazawa, H.; Ohnishi, H. Protein tyrosine phosphatase SHP-2: a proto-oncogene product that promotes Ras activation. *Cancer Sci.* **2009**, *100*, 1786−1793.

(6) Chong, Z. Z.; Maiese, K. The Src homology 2 domain tyrosine phosphatases SHP-1 and SHP-2: diversified control of cell growth, inflammation, and injury. *Histol. Histopathol.* **2007**, *22*, 1251−1267.

(7) Wu, X.; Guan, S.; Lu, Y.; et al. Macrophage-derived SHP-2 inhibits the metastasis of colorectal cancer via Tie2-PI3K signals. *Oncol. Res.* **2023**, *31*, 125−139.

(8) Wei, Q.; Luo, S.; He, G. Mechanism study of tyrosine phosphatase shp-1 in inhibiting hepatocellular carcinoma progression by regulating the SHP2/GM-CSF pathway in TAMs. *Sci. Rep.* **2024**, *14*, 9128.

(9) Dose Finding Study of TNO155 in Adult Patients with Advanced Solid Tumors. *ClinicalTrials.gov*, 2024. NCT03114319. https://www.clinicaltrials.gov/ct2/show/NCT03114319?term=SHP2&rank=5.

(10) Phase Ib Study of TNO155 in Combination with Spartalizumab or Ribociclib in Selected Malignancies. *ClinicalTrials.gov*, 2024. NCT04000529. https://www.clinicaltrials.gov/ct2/show/NCT04000529?term=TNO155&rank=2.

(11) Dose Escalation of RMC-4630 Monotherapy in Relapsed/Refractory Solid Tumors. *ClinicalTrials.gov*, 2022. NCT03634982. https://www.clinicaltrials.gov/ct2/show/NCT03634982?term=SHP2&draw=2&rank=12.

(12) Dose-Esc/Exp RMC4630 & Cobi in Relapsed/Refractory Solid Tumors & RMC4630& Osi in EGFR+ Locally Adv/Meta NSCLC.

ClinicalTrials.gov, 2023. NCT03989115. https://www.clinicaltrials.gov/ct2/show/NCT03989115?term=RMC-4630&rank=2.
(13) A First in Human, Dose Escalation Study of JAB-3068 (SHP2 Inhibitor) in Adult Patients With Advanced Solid Tumors. *ClinicalTrials.gov*, 2021. NCT03518554. https://www.clinicaltrials.gov/ct2/show/NCT03518554?term=NCT03518554&rank=1.
(14) A First-in-human Study of JAB-3068 (SHP2 Inhibitor) in Adult Patients with Advanced Solid Tumors in China. *ClinicalTrials.gov*, 2024. NCT03565003. https://www.clinicaltrials.gov/ct2/show/NCT03565003?term=SHP2&draw=2&rank=1.
(15) A First-in-Human, Phase 1 Study of JAB-3312 in Adult Patients With Advanced Solid Tumors. *ClinicalTrials.gov*, 2022. NCT04045496. https://www.clinicaltrials.gov/ct2/show/NCT04045496?term=SHP2&rank=10.
(16) Liu, Q.; Qu, J.; Zhao, M.; Xu, Q.; Sun, Y. Targeting SHP2 as a promising strategy for cancer immunotherapy. *Pharmacol. Res.* **2020**, *152*, No. 104595.
(17) Chen, Y. N.; LaMarche, M. J.; Chan, H. M.; et al. Allosteric inhibition of SHP2 phosphatase inhibits cancers driven by receptor tyrosine kinases. *Nature.* **2016**, *535*, 148−152.
(18) Kocaadam, B.; Şanlier, N. Curcumin, an active component of turmeric (Curcuma longa), and its effects on health. *Crit. Rev. Food. Sci. Nutr.* **2017**, *57*, 2889−2895.
(19) Man, S.; Yao, J.; Lv, P.; Liu, Y.; Yang, L.; Ma, L. Curcumin-enhanced antitumor effects of sorafenib via regulating the metabolism and tumor microenvironment. *Food. Funct.* **2020**, *11*, 6422−6432.
(20) Peng, Y.; Ao, M.; Dong, B.; Jiang, Y.; Yu, L.; Chen, Z.; Hu, C.; Xu, R. Anti-Inflammatory Effects of Curcumin in the Inflammatory Diseases: Status, Limitations and Countermeasures. *Drug. Des. Devel. Ther.* **2021**, *15*, 4503−4525.
(21) Zheng, Q. T.; Yang, Z. H.; Yu, L. Y.; Ren, Y. Y.; Huang, Q. X.; Liu, Q.; Ma, X. Y.; Chen, Z. K.; Wang, Z. B.; Zheng, X. Synthesis and antioxidant activity of curcumin analogs. *J. Asian. Nat. Prod. Res.* **2017**, *19*, 489−503.
(22) Pricci, M.; Girardi, B.; Giorgio, F.; Losurdo, G.; Ierardi, E.; Di Leo, A. Curcumin and Colorectal Cancer: From Basic to Clinical Evidences. *Int. J. Mol. Sci.* **2020**, *21*, 2364.
(23) Kim, H. Y.; Park, E. J.; Joe, E. H.; Jou, I. Curcumin suppresses Janus kinase-STAT inflammatory signaling through activation of Src homology 2 domain-containing tyrosine phosphatase 2 in brain microglia. *J. Immunol.* **2003**, *171*, 6072−6079.
(24) Saydmohammed, M.; Joseph, D.; Syed, V. Curcumin suppresses constitutive activation of STAT-3 by up-regulating protein inhibitor of activated STAT-3 (PIAS-3) in ovarian and endometrial cancer cells. *J. Cell Biochem.* **2010**, *110*, 447−456.
(25) Xin, P.; Xu, X.; Deng, C.; et al. The role of JAK/STAT signaling pathway and its inhibitors in diseases. *Int. Immunopharmacol.* **2020**, *80*, No. 106210.
(26) Zou, S.; Tong, Q.; Liu, B.; Huang, W.; Tian, Y.; Fu, X. Targeting STAT3 in Cancer Immunotherapy. *Mol. Cancer.* **2020**, *19*, 145.
(27) Hung, C. M.; Su, Y. H.; Lin, H. Y.; et al. Demethoxycurcumin modulates prostate cancer cell proliferation via AMPK-induced down-regulation of HSP70 and EGFR. *J. Agric. Food. Chem.* **2012**, *60*, 8427−8434.
(28) Dei Cas, M.; Ghidoni, R. Dietary Curcumin: Correlation between Bioavailability and Health Potential. *Nutrients.* **2019**, *11*, 2147.
(29) Jabczyk, M.; Nowak, J.; Hudzik, B.; Zubelewicz-Szkodzińska, B. Curcumin and Its Potential Impact on Microbiota. *Nutrients.* **2021**, *13*, 2004.
(30) Górnicka, J.; Mika, M.; Wróblewska, O.; Siudem, P.; Paradowska, K. Methods to Improve the Solubility of Curcumin from Turmeric. *Life (Basel).* **2023**, *13*, 207.
(31) Štěpnička, P. Forever young: the first seventy years of ferrocene. *Dalton. Trans.* **2022**, *51*, 8085−8102.
(32) Santos, M. M.; Bastos, P.; Catela, I.; Zalewska, K.; Branco, L. C. Recent Advances of Metallocenes for Medicinal Chemistry. *Mini. Rev. Med. Chem.* **2017**, *17*, 771−784.
(33) Biot, C.; Glorian, G.; Maciejewski, L. A.; Brocard, J. S.; Domarle, O.; Blampain, G.; Millet, P.; Georges, A. J.; Abessolo, H.; Dive, D.; Lebibi, J. Synthesis and antimalarial activity in vitro and in vivo of a new ferrocene-chloroquine analogue. *J. Med. Chem.* **1997**, *40*, 3715−3718.
(34) Top, S.; Vessières, A.; Leclercq, G.; Quivy, J.; Tang, J.; Vaissermann, J.; Huché, M.; Jaouen, G. Synthesis, biochemical properties and molecular modelling studies of organometallic specific estrogen receptor modulators (SERMs), the ferrocifens and hydroxyferrocifens: evidence for an antiproliferative effect of hydroxyferrocifens on both hormone-dependent and hormone-independent breast cancer cell lines. *Chemistry.* **2003**, *9*, 5223−5236.
(35) Top, S.; Tang, J.; Vessières, A.; Carrez, D.; Provot, C.; Jaouen, G. Ferrocenyl hydroxytamoxifen: a prototype for a new range of oestradiol receptor site-directed cytotoxics. *Chemical Communications.* **1996**, 955−956.
(36) Arezki, A.; Chabot, G.; Quentin, L.; Scherman, D.; Jaouen, G.; Brulé, E. Synthesis and biological evaluation of novel ferrocenyl curcuminoid derivatives. *Medchemcomm.* **2011**, *2*, 190−195.
(37) Cai, P.; Guo, W.; Yuan, H.; et al. Expression and clinical significance of tyrosine phosphatase SHP-2 in colon cancer. *Biomed. Pharmacother.* **2014**, *68*, 285−290.
(38) Wang, Q.; Bode, A. M.; Zhang, T. Targeting CDK1 in cancer: mechanisms and implications. *NPJ. Precis. Oncol.* **2023**, *7*, 58.
(39) Noorolyai, S.; Shajari, N.; Baghbani, E.; Sadreddini, S.; Baradaran, B. The relation between PI3K/AKT signalling pathway and cancer. *Gene.* **2019**, *698*, 120−128.
(40) Zong, Y.; Zhou, Y.; Liao, B.; Liao, M.; Shi, Y.; Wei, Y.; Huang, Y.; Zhou, X.; Cheng, L.; Ren, B. The Interaction Between the Microbiome and Tumors. *Front Cell Infect Microbiol.* **2021**, *11*, No. 673724.
(41) Vilgelm, A. E.; Richmond, A. Chemokines Modulate Immune Surveillance in Tumorigenesis, Metastasis, and Response to Immunotherapy. *Front Immunol.* **2019**, *10*, 333.
(42) Chainoglou, E.; Hadjipavlou-Litina, D. Curcumin in Health and Diseases: Alzheimer's Disease and Curcumin Analogues, Derivatives, and Hybrids. *Int. J. Mol. Sci.* **2020**, *21*, 1975.
(43) Li, S.; Yin, S.; Ding, H.; Shao, Y.; Zhou, S.; Pu, W.; Han, L.; Wang, T.; Yu, H. Polyphenols as potential metabolism mechanisms regulators in liver protection and liver cancer prevention. *Cell Prolif.* **2023**, *56*, No. e13346.
(44) Yang, H.; Du, Z.; Wang, W.; Song, M.; Sanidad, K.; Sukamtoh, E.; Zheng, J.; Tian, L.; Xiao, H.; Liu, Z.; Zhang, G. Structure-Activity Relationship of Curcumin: Role of the Methoxy Group in Anti-inflammatory and Anticolitis Effects of Curcumin. *J. Agric. Food. Chem.* **2017**, *65*, 4509−4515.
(45) Lestari, M. L.; Indrayanto, G. Curcumin. *Profiles Drug Subst. Excip. Relat. Methodol.* **2014**, *39*, 113−204.
(46) Prasad, D.; Praveen, A.; Mahapatra, S.; Mogurampelly, S.; Chaudhari, S. R. Existence of β-diketone form of curcuminoids revealed by NMR spectroscopy. *Food Chem.* **2021**, *360*, No. 130000.
(47) Lei, Y. J.; Bi, Y.; Jie, O. Y. Synthesis of some curcumin analogues under ultrasound irradiation. *Adv. Mater. Res.* **2011**, *332-334*, 1623−1626.
(48) Deck, L. M.; Hunsaker, L. A.; Vander Jagt, T. A.; Whalen, L. J.; Royer, R. E.; Vander Jagt, D. L. Activation of anti-oxidant Nrf2 signaling by enone analogues of curcumin. *Eur. J. Med. Chem.* **2018**, *143*, 854−865.
(49) Laali, K. K.; Rathman, B. M.; Bunge, S. D.; et al. Fluoro-curcuminoids and curcuminoid-BF2 adducts: Synthesis, X-ray structures, bioassay, and computational/docking study. *Journal of Fluorine Chemistry.* **2016**, *191*, 29−41.

https://doi.org/10.1021/acsomega.4c10629
ACS Omega 2024, 9, 51701−51718